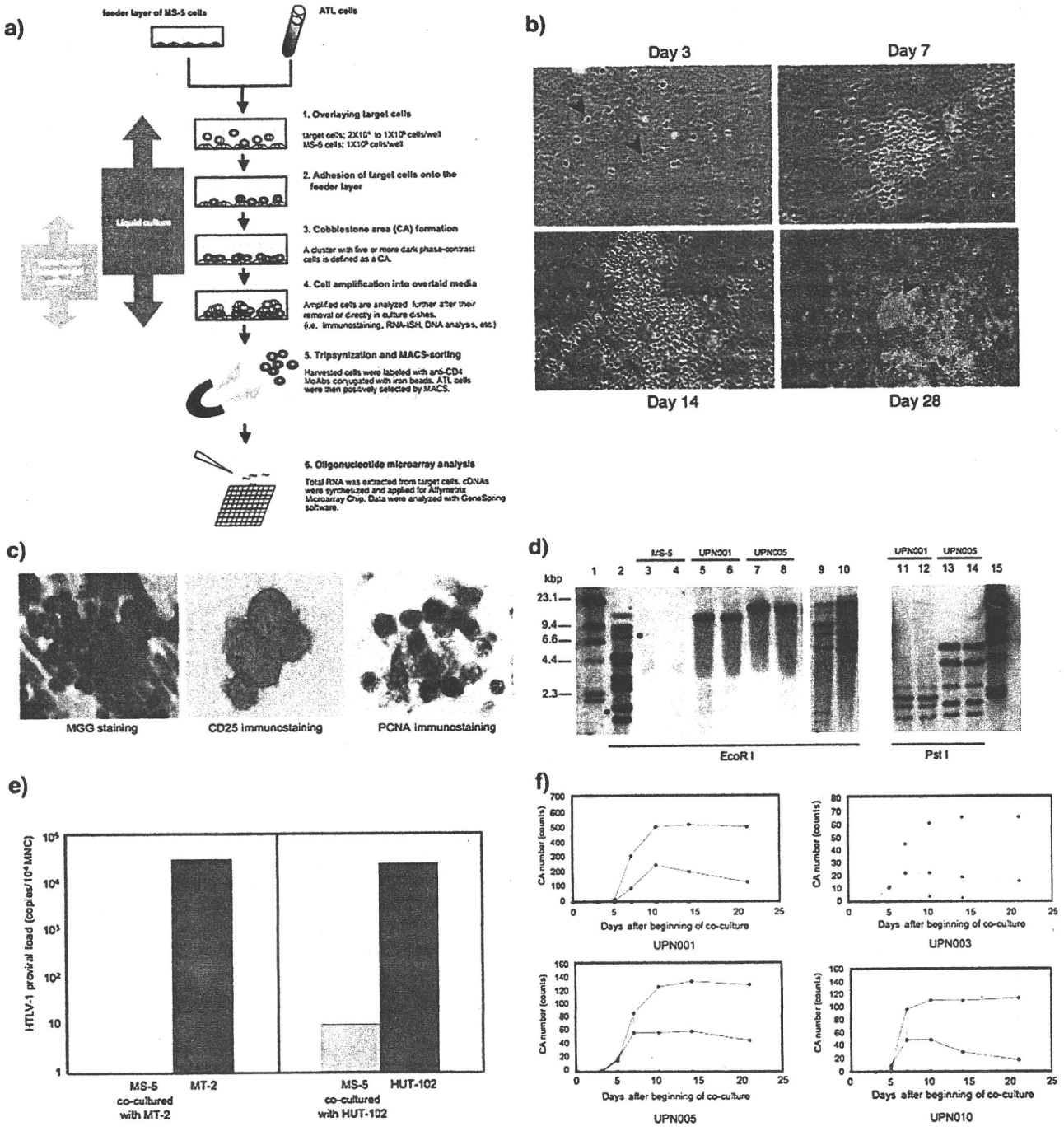

2.2 Monoclonal antibodies (MoAbs)

LT-4 (anti-p40Tax; mouse IgG_3) and Gin-7 (anti-p19Gag; mouse IgG2b) were used to detect Tax and Gag protein, respectively, by immunocytochemical staining [21, 22]. Leu3a (anti-CD4), Leu2a (anti-CD8), anti-Tac (anti-CD25), and PC-10 (anti-proliferating cell nuclear antigen (PCNA); DAKO Cytomation) were also used for immunophenotyping.

2.3 Co-culture system with a stromal layer of MS-5 cells

Murine marrow stromal MS-5 cells were kindly provided by Kirin Brewery Co. Ltd (Gunma, Japan). This cell line was originally established by Itoh et al. [17]. Maintenance of MS-5 cells and preparation of stromal feeder layers for co-culture experiments were as described previously [18]. The co-culture experiments are outlined in Fig. 1a. In short,

target cells were overlayed at various concentrations (2×10^4 to 1×10^5 cells/35 mm well) in RPMI1640 medium, including 20% fetal bovine serum (FBS), onto the feeder layer of MS-5 cells. The culture medium was changed twice a week. The culture dishes were observed daily under a phase-contrast microscope, and after an adequate period, cultured cells were processed in the following experiments.

In order to compare the capacity of target cell growth with the MS-5-stromal layer, co-culture experiments with HESS-5, which can support human hematopoietic cells in in vitro culture [23], or human umbilical venous endothelial cells (HUVEC) were performed. The murine marrow stroma cell line HESS-5 was kindly provided by the Pharmaceutical Frontier Research Laboratory, JT Inc. (Yokohama, Japan). HESS-5 cells were maintained in alpha-minimal essential medium (alpha-MEM; GIBCO) supplemented with 10% (v/v) horse serum (HS). HUVEC was purchased from Bio-Whittaker Inc., MD, USA, and maintained in accordance with the manufacturer's instructions.

In a few experiments, 2×10^5/mL ATL cells were cultured in RPMI1640 containing 20% FBS and 200 ng/mL recombinant human IL-2 (R&D systems) for five to seven days without any stromal feeder layers (liquid culture) for comparison studies with the co-culture system.

Strictly, to test the plating efficiency of primary ATL cells, we employed the Cellmatrix™ (Nitta gelatin Inc., Osaka, Japan) collagen gel culture kit according to the manufacturer's instructions. After verifying the formation of cellular clusters in a semi-solid state, these were counted under a phase-contrast microscope.

2.4 Immunocytostaining

Cells cultured on multi-chamber BioCoat/FALCON Culture Slides™ (Falcon Labware) were washed with phosphate-buffered saline (PBS). In some experiments, cytospin preparations were made from colony-composing cells and from liquid cultures. For immunostaining CD4, CD8, CD25, PCNA, and HTLV-1-related proteins, preparations were fixed with appropriate fixatives for each antigens, incubated with primary antibodies, and stained using the streptavidin–biotin-alkaline phosphatase-labeling method or the diaminobenzidine tetrahydrochloride-based horse-radish peroxidase reaction as described previously [24, 25]. To estimate the positive staining rate, a minimum of 200 ATL cells was observed under a light microscope with a final magnification of 1,000× (Nikon, Japan).

2.5 Southern blot hybridization (SBH) and HTLV-1 proviral load

The pattern of integration of the HTLV-1 provirus into the host genome was investigated using SBH as described previously [26]. In short, first, ATL cells, which proliferated in the co-culture system, were harvested by trypsinization. Cell suspension was collected from culture vessels, and subsequently left to settle for 30 min at 37°C in fresh flasks, which allowed for the separation of ATL cells from adherent MS-5 cells onto the bottom of the flasks. After harvesting the supernatant, which included many ATL cells, and MS-5 cells, separately, genomic DNA was extracted from them. Aliquots of DNA were digested with restriction enzyme of *Eco*RI or *Pst*I, and then processed for SBH using a digoxigenin-labeled whole HTLV-1.

HTLV-1 proviral load was quantified using a real-time DNA PCR LightCycler Technology System according to our previously described method [27]. The sample copy number was estimated by interpolation from the standard curve generated by serial dilution of a *tax*-containing plasmid.

2.6 Cell adhesion blockade analysis

To inhibit the adhesion of ATL cells to the MS-5 monolayer, a Cell Culture Insert™ membrane (Falcon) with 0.4 μm pore size, on which 5×10^4 target cells were overlayed in methylcellulose including 20%FBS/RPMI1640, was inserted into the 35 mm culture well with the MS-5 monolayer on the bottom of each dish. In some experiments of this setting, 20%FBS/RPMI1640 was substituted for conditioned medium (CM), which was harvested from co-culturing of MT-2 and MS-5 layer.

2.7 RNA in situ hybridization (ISH)

The mRNA expression of the HTLV-I *tax* gene was investigated by ISH using a synthetic single-stranded 40-base oligonucleotide probe corresponding to 7409-7453 of this genetic region. The sequences of the oligo-DNA probes were as follows [28]: antisense probe for *tax* mRNA: 3′-ACGCCCTACTGGCCACCTGTCCAGAGCATCAGA TCACCTG-5′, sense probe for *tax* mRNA: 3′-TGCG GGATGACCGGTGGACAGGTCTCGTAGTCTAGTGG AC-5′, and antisense probe for 28S ribosomal RNA as an internal control: 3′-TGCTACTACCACCAAGATCTGCA CCTGCGGCGGC-5′. These probes were conjugated with digoxigenin (DIG) at 3′. Unstained cytospin preparations and cultured chamber-slides were fixed for 10 min in 2% paraformaldehyde/PBS at room temperature. Subsequently, fixed preparations were processed using the Ventana HX Discovery™ (Ventana Medical Systems, Tucson, AZ) automated ISH instrument system according to the manufacturer's instructions. The conditions of each reaction were as follows: denaturation; for 10 min at 42 °C for 10 min, hybridization with oligo-probe; for 6 h at 37 °C, incubation with secondary antibody; for 30 min at 37 °C, and

colorization in streptavidin-conjugated HRP solution; for 90 min at 37 °C. The expression of the Tax gene was evaluated using a light microscope (Nikon, Japan) with a final magnification of 1,000×. A minimum of 200 ATL cells was observed in each specimen to estimate the positive staining rate. ATL cells were considered to have expressed the Tax gene when they displayed a blue–gray signal in their cytoplasm or nucleus.

2.8 Oligonucleotide microarray analysis

$CD4^+$ ATL cells were harvested from the co-culture system by trypsinization, and purified by MACS magnetic cell separation system (Miltenyi Biotec) immediately. Primary samples were also processed as described above, except for trypsinization. Enrichment of the $CD4^+$ fraction was evaluated by subjecting portions of MNC and $CD4^+$ cell preparations to analysis of the expression of CD4 by flow cytometry (FACSCaliber™; Becton-Dickinson, Mountain View, CA, USA). In all samples, the $CD4^+$ fraction constituted greater than 90% of the eluate of the affinity column. Total RNA was isolated from CD4-positive ATL cells using TRIzol reagent as described by the manufacturer (Life Technologies, Inc., Gaithersberg, MD), and then treated with RNase-free DNase I (RQ1 DNase) at 37 °C for 30 min (Promega, Madison, WI). The preparation of RNA and hybridization with HGU133A & B microarrays (Affymetrix, Santa Clara, CA, USA) were as described previously [29].

2.9 Quantification of mRNA levels using real-time PCR

Total RNA was used for cDNA synthesis using Oligo(dT)12–18 Primer (Invitrogen) and SuperScript TM3 Reverse Transcriptase (Invitrogen). Real-time PCR (*Taq*-Man) analysis was performed on a LightCycler (Roche) according to the manufacturer's instructions. Primers used for the validation studies of expression profiles are shown in Table 3. Experiments were performed with triplicates for each sample, and the glyceraldehydes-3 phosphate dehydrogenase (GAPDH) expression was used to normalize the expression of each gene for sample-to-sample differences in RNA input, RNA quality and reverse transcriptase efficiency. Furthermore, quantification of mRNA levels of HTLV-I basic leucine zipper factor (HBZ) and Tax genes was performed as described previously [30]. Assays were carried out in duplicate and the average value was used as absolute amounts of HBZ and Tax mRNA in samples.

2.10 Statistical analysis

The Mann–Whitney *U* test and Student's *t* test were used for statistical analysis with StatView software. To analyze the data of microarray analysis, the fluorescence intensity of each gene was normalized relative to the median fluorescence value for all human genes with a "Present" and "Marginal" call (Microarray Suite; Affymetrix) in each hybridization. Comparative analysis by fold change data was performed with GeneSpring 7.0 software (Silicon Genetics, Redwood, CA, USA).

3 Results

3.1 Growth of ATL cells in co-culture system with MS-5

HTLV-1-transformed and ATL patient-derived cell lines grew in close contact with the stromal layer of MS-5 cells and formed so-called "cobblestone areas" (CAs), which were made up of dark-contrasted clusters of growing cells under phase-contrast microscopy [31], without any exogenous cytokines. Not only IL-2-independent cell lines (MT-2, HUT-102, and OMT), but also two of three IL-2-dependent cell lines in our series, ST-1 and KOB, formed CAs without the addition of IL-2. KK-1 showed minimal growth in this culture system without IL-2.

Next, ATL cells from clinical samples were also used in this co-culture system. In representative cases, which showed prosperous growth, ATL cells adhered and crept into the stromal layer in a few days from the start of co-culture, grew with formation of CAs from day 10 to 14, and continued to grow over three weeks and proliferated upward into the medium out of CA cells in the third or fourth week of co-culture (Fig. 1b). In eight of 10 (80.0%) samples of acute ATL and one sample of lymphoma type, CA formation was observed, whereas three samples from two patients with chronic type of ATL, one with smoldering type and the control peripheral T cells obtained from healthy volunteers with Con-A stimulation did not have CA-forming cells (Table 1).

In May-Grunwald-Giemsa (MGG) staining, growing cells in CAs showed small lymphocyte-type morphology with convoluted nuclei as primary ATL cells show, although some growing cells showed immature, namely blastic features, which differed from primary malignant cells in the peripheral blood obtained from the patients. Immunostaining of CD4 and CD8 revealed that these cells had the immunophenotype of helper T cells, which were identical to primary ATL cells. Furthermore, since PCNA immunostaining in CA-composing cells from ATL showed a positive reaction, these cells were assumed to be in a growth phase (Fig. 1c). In two cases (UPN001 and 005), SBH analysis revealed that the integration pattern of the HTLV-1 provirus in ATL cells composing CA in each case was identical to that in primary ATL cells (Fig. 1d).

Table 1 Proliferation assay of primary ATL cells co-cultured with MS-5 cells

UPN	Subtype	Material	Frequency of clonogenic cells (%)		
			CAFC	Colony formation	
				IL-2 (+)[a]	IL-2 (–)
001	Acute	PE	1.04	0	0
		PB	0.78	0	0
002	Acute	PB	0	0	0
003	Acute	LN	0.32	0	0
004	Acute	PB	0.03	0	0
		LN	0.05	0	0
005	Acute	PB	0.12	0	0
006	Acute	PB	0.08	0	0
007	Acute	PB	0.25	0	0
008	Acute	LN	0.31	0	0
009	Acute	PB	0	0	0
010	Acute	LN	0.25	0	0
011	Lymphoma	LN	0.68	0	0
012	Chronic	PB	0	0.034	0
013	Chronic	PB	0	0.012	0
014	Chronic	PB	0.014	0.031	0
015	Smoldering	PB	0	0	0
016	Healthy[b]	PB	0	nd	nd
017	Healthy[b]	PB	0.008	nd	nd

PB peripheral blood, *LN* lymph node, *PE* pleural effusion

[a] Concentration of IL-2 was 200 ng/ml

[b] Con-A-stimulated (10 ng/ml) T cells were cultured

Table 2 Inhibitory effect of contact between ATL cells and stromal layer of MS-5

Sample	Frequency of clonogenic cells (%)						
	CAFC		Colony formation				
MS-5 stroma	+	+	+	+	+	–	–
Contact inhibition[a]	–	–	+	+	+	–	–
Co-cultured CM[b]	–	–	–	+	–	+	–
Exogenous IL-2[c]	–	+	–	–	+	–	+
UPN005 (acute)	0.12	0.21	0	0	0	0	0
UPN006 (acute)	0.08	0.06	0	0	0	0	0
UPN007 (acute)	0.25	0.24	0	0	0	0	0
UPN009 (chronic)	0	0.08	0	0.08	0	0	0.08

[a] A CellCulture Insert™ membrane was inserted to the co-culture system to inhibit direct cell–cell interaction between ATL cells and MS-5 cell layer. Values represent frequency of CAFC or colony-forming unit in the co-culture system and in the co-culture system with contact inhibition or in conditions without a MS-5 layer, respectively

[b] In this condition, we added conditioned medium (CM) which was harvested from co-culturing of MT-2 and MS-5 layer

[c] Concentration of IL-2 was 200 ng/ml

3.2 Significance of adhesion of ATL cells to stromal layer

A contact-inhibition experiment with a Cell Culture Insert™ membrane inserted in culture dishes was performed for four cases (three cases of acute type and one case of chronic type). In all three acute cases, CAs formed only under conditions, which allowed for close contact with the stromal layer of MS-5 cells. There was no colony formation in methylcellulose semi-solid cultures under contact inhibition to the stromal layer using Cell Culture Insert™, or without a stromal layer, regardless of stimulation by exogenous IL-2 or co-cultured CM. In a chronic subtype, although there was no CA formation in this co-culture system, colony formation was observed with IL-2 stimulation (Table 2). SBH analysis and quantification studies of HTLV-1 viral load revealed that infection of HTLV-1 to MS-5 cells was not detected in co-culturing with MT-2, although slightly detected in co-culturing with HUT-102 (Fig. 1d, e).

Compared with the MS-5 stromal layer, significantly less CA formed in co-culture with the HESS-5 stromal layer after day 7 of co-culturing, although we could observe comparable adhesion and growth of target cells on both stromal layers at earlier phase. Furthermore, there was no sustainable CA formation in co-culture with HUVEC (Fig. 1f). We applied the co-culture system with the MS-5 stromal layer in further analysis because of its superior efficiency for CA formation.

The semi-solid collagen gel culture of five primary ATL samples [UPN001 (PB), 003, 005, 007, and 011] revealed a linear relationship between the inoculated cell number and CA count, indicating that this assay system would be useful to quantify clonogenic precursors of ATL cells, i.e., CA-forming cells (CAFC) (Fig. 2a; Table 1). In our series, the frequency of CAFC in acute or lymphoma type varied considerably, ranging from 0.03 to 1.04% (median 0.25), and was significantly higher than in chronic type or healthy donors ($P < 0.01$; Fig. 2b).

3.3 HTLV-1 proviral gene expression in neoplastic CAs

The production of Tax and Gag proteins in ATL cells co-cultured with a stromal layer were examined by immunostaining and ISH. Based on immunostaining, these proteins seemed to disappear in CAs in ATL cell lines, HUT-102 and ST-1 (Fig. 3a).

Four cases of acute-type ATL showed a strong staining pattern for these proteins in primary neoplastic cells after liquid culture with stimulation by IL-2; however, ATL cells in CA showed significantly weaker staining for Tax and Gag proteins in all four cases (Fig. 3b). Furthermore, in

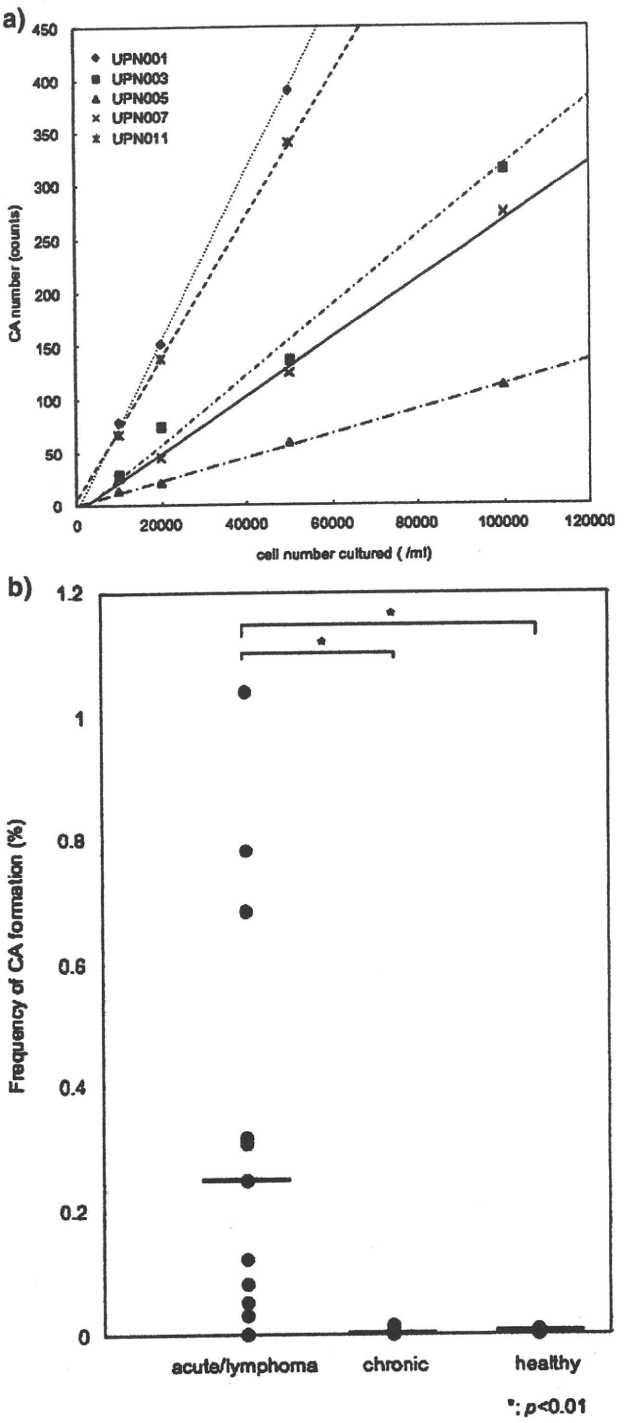

Fig. 2 Plating efficiency of ATL cells in a co-culture system with MS-5 cells. **a** The frequency of CA-forming cells (CAFC) of five cases (UPN001 (PB), 003, 005, 007, and 011) was examined with semi-solid collagen gel in the co-culture system. A clear linear relationship was obtained between the inoculated cell number and CAFCs in all cases examined. **b** The distribution plots of frequency of CA formation in different sample group; There is statistical difference in the median (*horizontal bars*) among acute/lymphoma type (0.25%), chronic type (0%), and healthy volunteers (0.04%) ($P < 0.01$)

three cases of acute ATL, the results of ISH revealed that the expression of the Tax gene of ATL cells in CA was markedly decreased when compared with that of growing cells in liquid culture with IL-2 (Fig. 3c).

Next, we quantified the expression level of HBZ gene, which was recently identified in the 3″-LTR of the complementary sequence of HTLV-1 and has been suggested as a critical gene in leukemogenesis of ATL [6, 32, 33]. As shown in Fig. 3d, the HBZ gene was highly expressed in MT-2 cells in CA, and the level of mRNA load was equivalent to those without co-culturing. With regard to *tax* gene, the expression level was significantly higher in cells in liquid culture without stroma than in cells in CA, although the difference was not so striking as observed in RNA-ISH analysis. Moreover, in the contact-inhibited condition to the stromal layer, the expression levels of these two genes were comparable to those without co-culturing.

3.4 Gene expression profiles of ATL cells composing CA

Next, we compared the gene expression profiles of sets of ATL cells composing CA matched with their corresponding $CD4^+$ primary samples from the same individuals by high-density oligonucleotide microarray analysis, to search for candidates of disease-specific molecules and signaling pathways, which contribute to the mechanism of adhesion-dependent proliferation in our co-culture system. After removal of transcriptionally silent genes from the analysis of 44,764 probe sets using Microarray Suite software, Student's *t* test ($P < 0.001$) was then used to extract genes, the expression level of which significantly differed between cells in CA and primary samples. Genes were considered up- or down-regulated if each value and the average fold change were 3.5 or greater in all three data sets. Finally, we could identify 110 and 98 genes significantly up- and down-regulated in ATL cells in CA compared with primary samples by selecting genes based on the reproducibility, respectively (Fig. 4a).

To validate the microarray findings, we performed RTQ-PCR for eight genes that were significantly up- or down-regulated in ATL cells in CA of three-paired array samples, and with code products correlating with adhesion molecules and cell–cell interaction or with cellular apoptosis and proliferation. All experiments were performed in triplicate. Variance among triplicates was less than 5%. Standard curves with correlation coefficiency greater than 0.970 were produced from the data for each gene, indicating the large dynamic range and accuracy of RTQ-PCR (data not shown). As shown in Table 3 and Fig. 4b, we confirmed that these genes were actually up- or down-regulated in ATL cells in CA, compared with primary

neoplastic cells as indicated in the microarray data. Up-regulated genes, *CDH11* [34], *Twist1* [35] and *Cav-1* [36], are considered to play a major role in tumor promotion, progression, survival and metastasis in several neoplasias. Furthermore, the down-regulation of several genes, *hCdc14A* [37], *CUGBP2* [38], *HBP1* [39], and *ZNFN1A1* [40], the products of which are recognized to play a role in suppressing carcinogenesis through various signaling pathways, were also confirmed in ATL cells in CA.

4 Discussion

In the present study, we established a new ATL cell/murine stroma cell co-culture system with which we could observe the proliferation of primary ATL cells without any additional growth factor. In previous studies, primary ATL cells were able to grow in a liquid culture containing IL-2; however, they showed only a transient and cytokine-dependent proliferation [8–10]. On the other hand, we also observed involvement of HTLV-1 genome to patients' LN stroma cells and production of several cytokines from them [16]. In the present study, infection of HTLV-1 to MS-5 was considered to be dispensable to adhesion-dependent ATL cell growth, as shown in the negative or minimal viral load in co-cultured MS-5 cells. Furthermore, since many murine cytokines cannot affect human cells [41], and especially in this co-culture system, any soluble factor or co-cultured CM did not stimulate ATL cells growth in the contact-inhibition test, direct adhesion of target cells to the stromal layer of MS-5 layers are considered to be essential for CA formation by primary ATL cells in this co-culture system.

In the lymphohematopoietic microenvironment, normal and neoplastic lymphoid cells are affected by various molecules [42, 43]. Concerning lymphoid malignancies, recent reports has indicated that interactions between neoplastic cells and BM or LN stromal cells regulate growth, survival, and homing in multiple myeloma, mantle cell lymphoma, and other non-Hodgkin lymphoma [44, 45]. Whereas, the expression of various adhesion molecules and chemokine receptors on leukemic cells, also in ATL, is assumed to be essential to the pathophysiology of this disease [46–50], the significance of these molecules in the growth and survival of ATL cells is still poorly understood. Thus, extensive investigation of the molecular interaction between neoplastic cells and lymphohematopoietic microenvironment is essential to clarify not only adhesion and transmigration, but also the growth and survival mechanism of primary ATL cells in this co-culture system.

In the present study, two murine stromal cell lines, MS-5 and HESS-5 showed significant supportive capacity on leukemic CA formation comparing with HUVEC, and also indicated their differential abilities for support of growth and survival of target cells. Both of them were originally established from C3H/HeN strain mice and might share common characters concerning the interaction between hematopoietic cells and stroma layer through integrin family members [51, 52]. Furthermore, target cells could adhere and start to grow on both stromal layers in our series. Our limited studies did not reveal the mechanism of differential abilities to support the growth of ATL cells between MS-5 and HESS-5 with respect to the direct interaction to target cells for the maintenance of CA formation. Previous reports concerning successful xeno-transplantation of ATL cells into immunodeficient mice indicated that indispensable extrinsic elements might be supplied to human neoplastic cells in these in vivo animal models sharing similarity with human lymphohematopoietic microenvironment [53, 54]. In analogy, our in vitro

Fig. 3 Expression of HTLV-1-related genes in ATL cells in CA. ▶ **a** HUT-102 and ST-1 cells were examined by phase-contrast micrographs (final magnification ×400), May-Giemsa staining (final magnification ×600), and immunostaining of Tax protein on ATL cells in CA and on cells after liquid culture using anti p40Tax antibody, Lt-4 (final magnification ×400). **b** Expression of HTLV-1 viral proteins on ATL cells in CA obtained from primary ATL cells. Four patients with acute-type ATL were examined. *Color* photographs show representative results of immunostaining of Tax (*upper*) and Gag (*lower*) in primary cells after culture with IL-2 for 7 days (*left*) and ATL cells in CA (*right*) (UPN004). *Bar graphs* are a summary of results of immunostaining of Tax and Gag protein in four cases. Light and *dark gray bars* indicate the results of primary ATL cells after liquid culture with IL-2 and those of ATL cells in CA in our co-culture system, respectively. Data are presented as the mean percentage of positive cells in triplicate experiments with error bars indicating 1SD. Mann–Whitney's *U* test was performed for statistical analysis and, in every sample, the positive rate of immunostaining of p19 and p40 was significantly lower in ATL cells in CA than in primary ATL cells after liquid culture with IL-2 ($P < 0.01$). **c** *tax* mRNA expression in ATL cells in CA obtained from primary ATL cells. ATL cells obtained from three cases were analyzed by RNA-ISH method. *Color* photographs show representative results of the analysis of UPN001; primary ATL cells after liquid culture with IL-2 (*left*) and ATL cells in CA (*right*): tested with the probe to 28S ribosomal RNA as an internal control (*upper*), the antisense oligonucleotide probe to the *tax* mRNA (*middle*), and the sense oligonucleotide probe (*lower*), indicated in "Sect. 2". Areas surrounded by arrowheads are CAs. *Bar graphs* are a summary of the results of three primary samples, which were analyzed RNA-ISH for *tax* mRNA. Light and dark gray bars indicate the results of primary ATL cells after liquid culture with IL-2 and those of ATL cells in CA in our co-culture system, respectively. Data are presented as the mean percentage of positive cells in triplicate experiments with error bars indicating 1SD. Mann–Whitney's *U* test was performed for statistical analysis and, in every sample, the positive rate of *tax* mRNA expression was significantly lower in ATL cells in CA than in primary ATL cells after liquid culture with IL-2 ($P < 0.01$). **d** Results of quantification of mRNA load of HBZ and *tax* genes. The copy number of target mRNA per 50 ng total RNA was estimated from the standard curves [29]. *Light* and *dark gray* and *white bars* indicate data, which were obtained from HUT-102 and MT-2 cell lines in three different culture conditions; conventional liquid culture, co-culture with MS-5, and contact-inhibited condition to MS-5 stromal layer, respectively

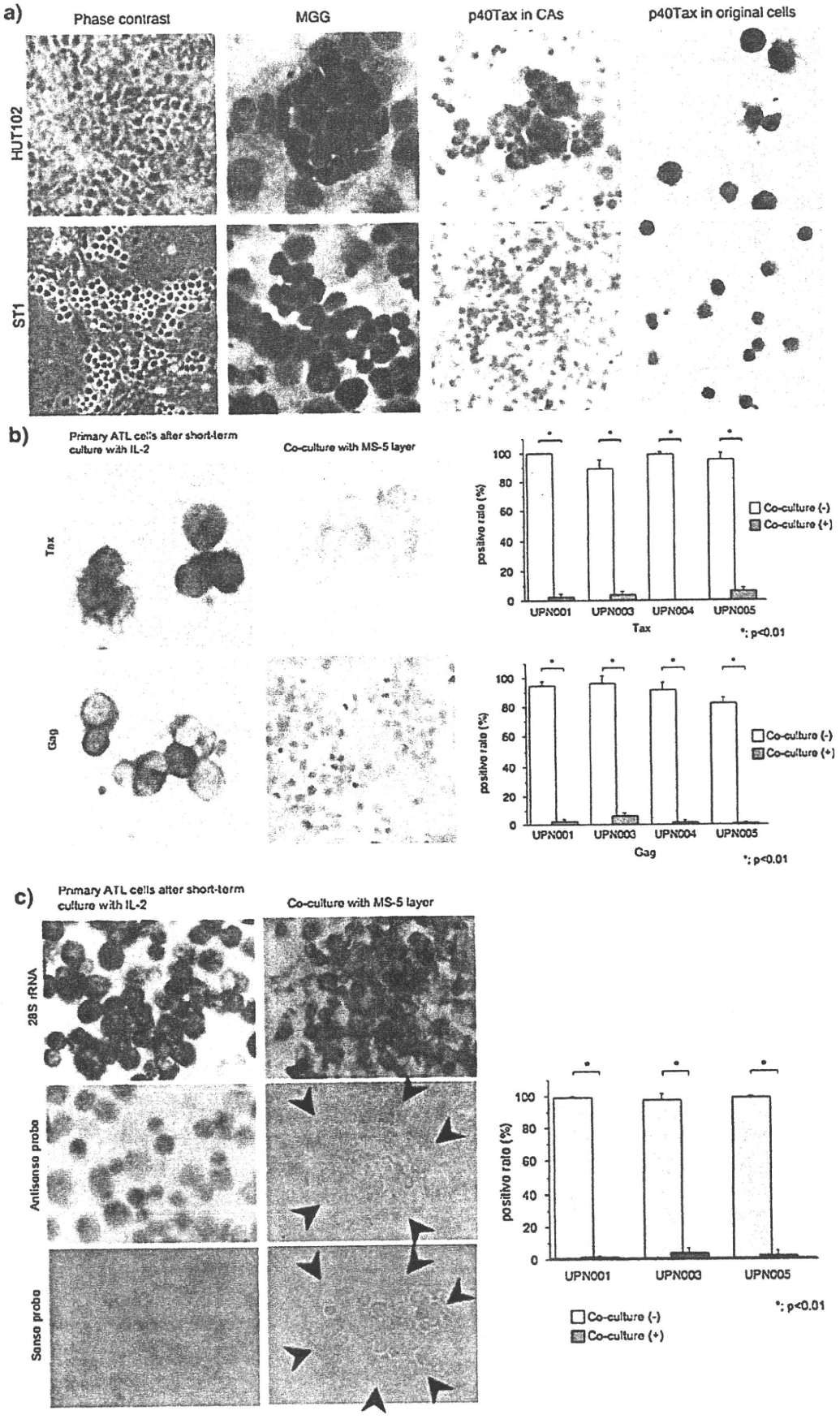
a)
Phase contrast
MGG
p40Tax in CAs
p40Tax in original cells
HUT102
ST1
b)
Primary ATL cells after short-term culture with IL-2
Co-culture with MS-5 layer
Tax
Gag
positive rate (%)
Co-culture (-)
Co-culture (+)
UPN001
UPN003
UPN004
UPN005
Tax
Gag
*: p<0.01
c)
Primary ATL cells after short-term culture with IL-2
Co-culture with MS-5 layer
28S rRNA
Antisense probe
Sense probe
positive rate (%)
UPN001
UPN003
UPN005
Co-culture (-)
Co-culture (+)
*: p<0.01

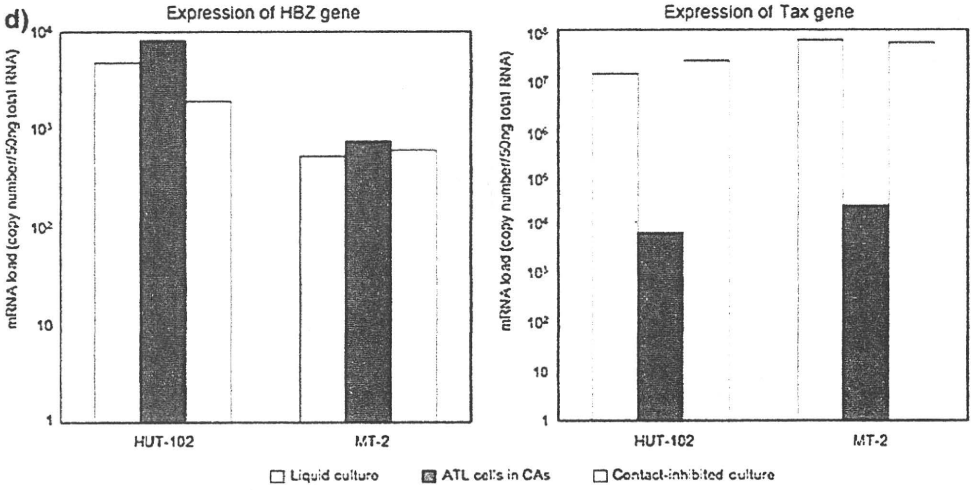

Fig. 3 continued

co-culture system is also considered to provide ATL cells with common factors with in vivo adhesion-dependent growth mechanism of ATL cells.

Although neoplastic cells of lymphoid malignancies have been considered to proliferate primarily in lymphoid tissues, there are so far few cell lines established from LN stroma and available for reproducible analysis of neoplastic cell growth. Since ATL cells frequently invade and proliferate in BM, especially in aggressive phase, this co-culture system is considered to provide components which are necessary for growth and survival of neoplastic cells in BM microenvironment. Surprisingly, we reported previously that in a semi-solid colony assay system, IL-2-dependent colony formation occurred in almost all cases of chronic or smoldering type, but rarely in acute and lymphoma types [55]. These results observed among our limited number of clinical cases indicate that in the prodromal phase of ATL, some cytokines were needed for the growth of neoplastic cells in vitro, while in a more aggressive phase, such a cytokine-dependency declines and some aberrant signal transducers might contribute to a more autonomous proliferation and enhance survival of ATL cells through anti-apoptotic process, which is considered to be closely related to stroma-dependent cell growth.

It has been demonstrated recently in several cancers, especially leukemias, that neoplastic cells are heterogeneous in terms of their capacity to grow and self renew, and that only a small proportion of cells are actually clonogenic in culture and also in vivo [56]. Many recent evidences indicate that microenvironment contributes significantly to tumorigenesis originated from such "cancer stem cells" [57]. In the present study, the leukemic CAFCs exhibited clonogenic potential by showing a linear relationship between inoculated ATL cells and CA numbers as carefully enumerated in the semi-solid collagen gel culture. Furthermore, in four of eight acute-type cases, which gave rise to primary growth, we could observe the secondary CA formation in replating experiments (data not shown). Although it remains controversial whether there exists such a hierarchy in a malignant clone of ATL, our observation supports the hypothesis that there might be a neoplastic stem cell system also in ATL, and future studies on the cellular biology of leukemic CAFCs would shed light on our knowledge of this concept, especially in the context of interaction with the microenvironment of lymphohematopoietic tissue. This is important in that any treatment modality must eradicate such clonogenic cells that are quiescent or proliferating in close contact with stromal cells to obtain a cure.

In the present study, immunostaining and RNA-ISH analysis revealed that our co-culture system allowed the growth of primary ATL cells even with a trace amount of Tax, at the level of transcription and translation. On the other hand, expression of HBZ gene in ATL cells was not affected by our co-culture system. Interestingly, this difference in expression pattern of two genes apparently resembles the behavior of ATL cells in vivo. Together with the result of mRNA load assay in the adhesion blockade system and the finding of reappearance of Tax protein in ATL cell lines which grew upward from the CAs and detached from the MS-5 monolayer into the culture medium (data not shown), it is suggested that there might be a direct interaction between ATL cells and stromal layer as a regulatory mechanism of *tax* gene expression, including epigenetic modification, in this co-culture system. Furthermore, we believe that further investigation of the actions of the *HBZ* gene in this unique in vitro culture system is important to clarify not only regulatory mechanism of *tax* gene expression [58], but also interactions between microenvironment and ATL

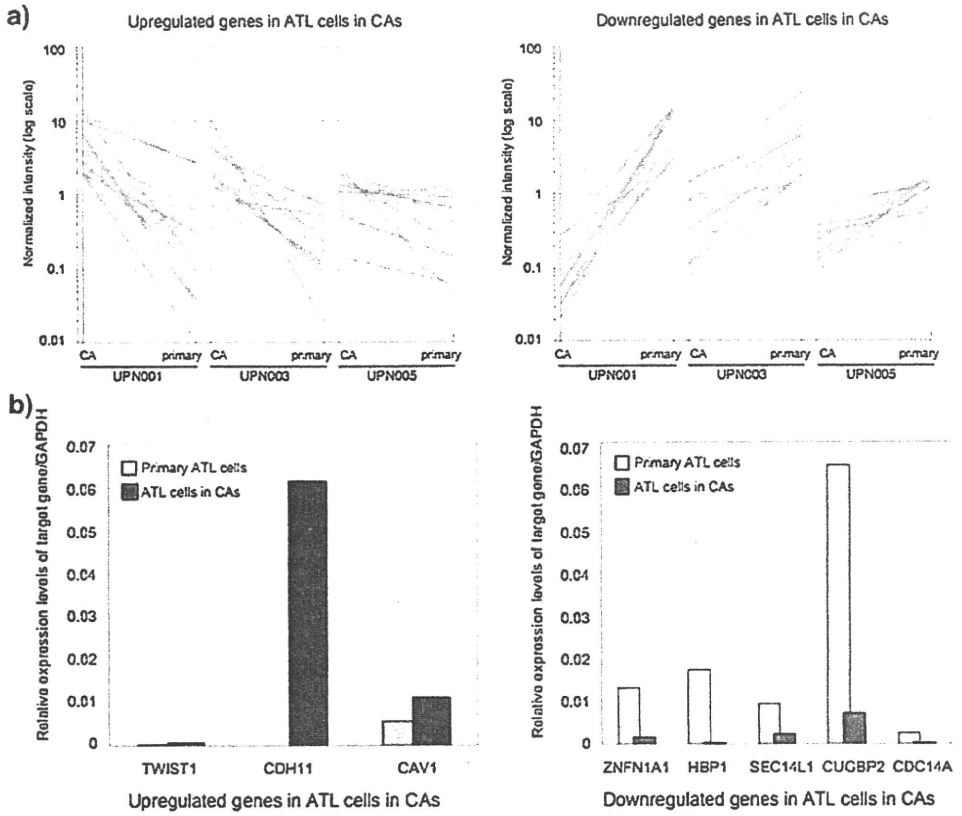

Fig. 4 Comparative studies of gene expression profiles between ATL cells in CA and corresponding primary cells from three clinical samples. For the expression data set of subjects, we first set a condition in which the expression level of a given gene should receive the "Present" call [from Microarray Suite 5.0 (Affymetrix)] in at least 60% (four samples) of the samples, aiming to remove transcriptionally silent genes from the analysis. The mean expression intensity of the internal positive control probe sets (http://www.affymetrix.com/support/technical/mask_files.affx) was set to 500U in each hybridization, and the fluorescence intensity of each test gene was normalized accordingly. **a** Diagrams of comparative profiles of three matched ATL cells in CA and their corresponding $CD4^+$ primary samples from the same individuals (UPN001, UPN003, and UPN005); up-regulated genes (*left*) and down-regulated genes (*right*) in ATL cells in CA. **b** Validation of the expression of eight selected genes from the expression profiles by RTQ-PCR. Primers and probes used in this study are shown in Table 3. Results are expressed in *graphs* of primary cells (*light gray bars*) and those of ATL cells in CA (*dark gray bars*) as fold differences between samples in their target gene expression relative to their levels of GAPDH. Standard curves were generated for each gene with tenfold serial dilution (100×10^{-6}) of cDNA from the KOB cell line and lymphocytes obtained from healthy volunteers. After confirming the precise log-linear relation of the standard curve, the final results were expressed as fold differences between samples in their target gene expression relative to their levels of GAPDH

cells for their growth and survival. This co-culture system is considered to be useful for the analysis of ATL cell growth and survival in a condition without excessive effect of Tax which was always present in the former in vitro culture systems.

Application of transcriptional profiling of ATL cells in CA revealed that there were no significant difference between ATL cells composing CA and primary ATL cells in expression level of several molecules, which play important roles in signaling pathways in ATL, including NFkB pathway. NFkB and related molecules have been shown to be constitutively activated in vivo without expression of Tax [59], although the mechanism of the constitutive activation of NFkB is still unclear. Therefore, several essential signaling pathways could also contribute to the growth of ATL cells under the adhesion-dependent and Tax-independent condition, which apparently resembles in vivo proliferation. On the other hand, interestingly also, we confirmed significant up- and down-regulation of several adhesion molecules and adaptor proteins, which play important roles in signaling pathways through cell-cell or cell-matrix interaction in ATL cells in CA. Taken together, these findings are assumed to indicate that our co-culture system might expose novel molecular mechanisms, which specifically regulate the growth and survival of clonogenic ATL cells. We believe that "outside-in" signaling pathways from interaction with the microenvironment might control such a mechanism in ATL cells. Further investigations are needed to elucidate the precise functions of these molecules.

Recently, a number of novel therapeutic agents to treat neoplastic diseases have been developed, as the growth

Table 3 Genes whose expressions were up- or down-regulated in ATL cells in CA compared with corresponding primary cells as determined by microarray analysis and validated by RTQ-PCR

Gene title	Genbank Accession ID	Description	Primers	Product size	Fold change
Upregulated genes in CAs					
CDH11	D21254	Osteoblast-cadherin	S CTGGAACCATTTTTGTGATT AS TCCACCGAAAAATAGGGTTG	343 bp	32.93
TWIST1	X99268	Twist-related protein 1, H-Twist, Twist homolog 1 (acrocephalosyndactyly 3; Saethre-Chotzen syndrome)	S GTCCGCAGTCTTACGAGGAG AS CCAGCTTGAGGGTCTGAATC	159 bp	5.026
CAV1	AU147399	Caveolin 1, caveolae protein	S CGCACACCAAGGAGATCGA AS GTGTCCCTTCTGGTTCTGCAAT	106 bp	5.301
Downregulated genes in CAs					
CDC14A	NM_003672	CDC14 cell division cycle 14 homolog A	S GCACTTACAATCTCACCATTC AS CATGTTGTAATCCCTTTCTG	58 bp	0.0748
CUGBP2	N36839	CUG triplet repeat, RNA binding protein 2	S CCTTTGAGGACTGCCATTGT AS TGAGGGGGAAAGTCCTTTTT	236 bp	0.0723
SEC14L1	AI017770	SEC14 like 1 protein	S TCCAAGAGGTCGCCACAACCAC AS AGAGACCTGCAGGGACGCAA	288 bp	0.0686
HBP1	AI689935	High mobility group (HMG) box transcription factor 1	S GCTTCCTTTGCAATGGTTCT AS CTGTGCAGCTCACATCTGTATG	243 bp	0.0646
ZNFN1A1	NM_018563	DNA-binding protein Ikaros, Zinc finger protein, subfamily 1A, 1	S CGAGTTCTCGTCGCACATAA AS ATCAAACCCCAATCAACCAA	221 bp	0.0571

Matching primers and fluorescence probes were designed for each of the genes selected by microarray data, employing PRIMER3 software (http://www.genome.wi.mit.edu/cgi-bin/primer/primer3_www.cgi) using sequence data from the NCBI database

mechanism of neoplastic cells becomes clearer at the molecular level. We have previously reported that this co-culture system could be used to test the sensitivity of neoplastic progenitors of Philadelphia chromosome (Ph^1)/BCR-ABL-positive leukemia to p210 tyrosine kinase inhibitor, imatinib mesylate (Gleevec^{TM}) [18]. This observation provides evidence that our co-culture system is extremely valuable for testing human tumor cells to grow using similar signaling pathways as in vivo. IL-2-dependent T cell lines established from a bulk liquid culture were usually clonally different from primary ATL cells [60], whereas our co-culture system exhibited growth of primary ATL cells which were identical clone to clinical samples as shown in SBH analysis, indicating the superiority of our method for the study of primary ATL cells as a surrogate assay system to predict response of neoplastic progenitors to therapeutic candidate drugs.

5 Conclusion

The present study showed that our newly established ATL cell/murine stroma cell co-culture system is highly efficient for the assay of primary ATL cell growth. Further investigation should focus on the elucidation of novel disease-specific signaling pathways starting from adhesion molecules and extracellular matrix proteins in this co-culture system, which contribute to adhesion-dependent proliferation and survival of ATL cells with a resemblance of expression pattern of proviral genes to that of in vivo ATL cells. This achievement might also be useful in developing novel therapeutic agents targeting ATL progenitors.

Acknowledgments The present study was supported by grants-in-aid from the Ministry of Education, Science and Culture of Japan (12670992) and by the twenty-first Century Center of Excellence (COE) Program of Nagasaki University "International Consortium for Medical Care of Hibakusha and Radiation Life Science".

References

1. Uchiyama T, Yodoi J, Sagawa K, Takatsuki K, Uchino H. Adult T cell leukemia: clinical and hematologic features of 16 cases. Blood. 1977;50:481–92.
2. Takatsuki K. Adult T-cell leukemia. Intern Med. 1995;34:947–52.
3. Yoshida M, Miyoshi I, Hinuma Y. Isolation and characterization of retrovirus from cell lines of human adult T-cell leukemia and its implication in the disease. Proc Natl Acad Sci USA. 1982;79:2031–5.
4. Yoshida M, Seiki M, Yamaguchi K, Takatsuki K. Monoclonal integration of human T-cell leukemia provirus in all primary tumors of adult T-cell leukemia suggests causative role of human

T-cell leukemia virus in the disease. Proc Natl Acad Sci USA. 1984;81:2534–7.
5. Arisawa K, Soda M, Endo S, Kurokawa K, Katamine S, Shimokawa I, et al. Evaluation of adult T-cell leukemia/lymphoma incidence and its impact on non-Hodgkin lymphoma incidence in southwestern Japan. Int J Cancer. 2000;85:319–24.
6. Yasunaga J, Matsuoka M. Leukaemogenic mechanism of human T-cell leukaemia virus type I. Rev Med Virol. 2007;17:301–11.
7. Aboud M, Golde DW, Bersch N, Rosenblatt JD, Chen IS. A colony assay for in vitro transformation by human T cell leukemia virus type 1 and type 2. Blood. 1987;70:432–6.
8. Uchiyama T, Hori T, Tsudo M, Wano Y, Umadome H, Tamori S, et al. Interleukin-2 receptor (Tac antigen) expressed on adult T cell leukemia cells. J Clin Invest. 1985;76:446–53.
9. Lunardi-Iskandar Y, Gessain A, Lam VH, Gallo RC. Abnormal in vitro proliferation and differentiation of T-cell colony forming cells in patients with tropical spastic paraparesis/human T lymphocyte virus type 1 (HTLV-1) associated myeloencephalopathy and healthy HTLV-1 carrier. J Exp Med. 1993;177:741–50.
10. Seiki M, Hattori S, Hirayama Y, Yoshida M. Human adult T-cell leukemia virus: complete nucleotide sequence of provirus genome integrated in leukemia cell DNA. Proc Natl Acad Sci USA. 1983;80:3618–22.
11. Yoshida M. Multiple viral strategies of HTLV-1 for dysregulation of cell growth control. Annu Rev Immunol. 2001;19:475–96.
12. Basbous J, Gaudray G, Devaux C, Mesnard JM. Role of the human T-cell leukemia virus type I Tax protein in cell proliferation. Recent Res Dev Mol Cell Biol. 2002;3:155–66.
13. Peloponese JM Jr, Kinjo T, Jeang KT. Human T-cell leukemia virus type 1 Tax and cellular transformation. Int J Hematol. 2007;86:101–6.
14. Kinoshita T, Shimoyama M, Tobinai K, Ito M, Ito S, Ikeda S, et al. Detection of mRNA for the tax1/rex1 gene of human T-cell leukemia virus type-1 in fresh peripheral blood mononuclear cells of adult T-cell leukemia patients and viral carriers by using the polymerase chain reaction. Proc Natl Acad Sci USA. 1989; 86:5620–4.
15. Ohshima K, Hashimoto K, Izumo S, Suzumiya J, Kikuchi M. Detection of human T lymphotropic virus type 1 (HTLV-1) DNA and mRNA in individual cells by polymerase chain reaction (PCR) in situ hybridization (ISH) and reverse transcription (RT)-PCR ISH. Hematol Oncol. 1996;14:91–100.
16. Joh T, Yamada Y, Seto M, Kamihira S, Tomonaga M. High establishment efficiency of lymph node stromal cells which spontaneously produce multiple cytokines derived from adult T-cell leukemia/lymphoma patients. Int J Oncol. 1996;9:619–24.
17. Itoh K, Tezuka H, Sakoda H, Konno M, Nagata K, Uchiyama T, et al. Reproducible establishment of hemopoietic supportive stromal cell lines from murine bone marrow. Exp Hematol. 1989;17:145–53.
18. Kawaguchi Y, Jinnai I, Nagai K, Yagasaki F, Yakata Y, Matsuo T, et al. Effect of a selective Abl tyrosine kinase inhibitor, STI571, on in vitro growth of BCR–ABL-positive acute lymphoblastic leukemia cells. Leukemia. 2001;15:590–4.
19. Maeda T, Yamada Y, Moriuchi R, Sugahara K, Tsuruda K, Joh T, et al. Fas gene mutation in the progression of adult T cell leukemia. J Exp Med. 1999;189:1063–71.
20. Shimoyama M, Members of the Lymphoma Study Group. Diagnostic criteria and classification of clinical subtypes of adult T-cell leukemia-lymphoma. A report from the Lymphoma Study Group. Br J Haematol (1984–1987) 1991;79:428–37.
21. Tanaka Y, Masuda M, Yoshida A, Shida H, Nyunoya H, Shimotohno K, et al. An antigenic structure of the trans-activator protein encoded by human T-cell leukemia virus type-1 (HTLV-1), as defined by a panel of monoclonal antibodies. AIDS Res Hum Retroviruses. 1992;8:227–35.
22. Tanaka Y, Lee B, Inoi T, Tozawa H, Yamamoto N, Hinuma Y. Antigens related to three core proteins of HTLV-I (p24, p19 and p15) and their intracellular localizations, as defined by monoclonal antibodies. Int J Cancer. 1986;37:35–42.
23. Tsuji T, Ogasawara H, Aoki Y, Tsurumaki Y, Kodama H. Characterization of murine stromal cell clones established from bone marrow and spleen. Leukemia. 1996;10:803–12.
24. Nagai K, Sohda H, Kuriyama K, Kamihira S, Tomonaga M. Usefulness of immunocytochemistry for phenotypical analysis of acute leukemia; improved fixation procedure and comparative study with flow cytometry. Leuk Lyphoma. 1995;16:319–27.
25. Adams JC. Heavy metal intensification of DAB-based HRP reaction products. J Histochem Cytochem. 1981;29:775.
26. Tsukasaki K, Ikeda S, Murata K, Maeda T, Atogami S, Sohda H, et al. Characteristics of chemotherapy-induced clinical remission in long survivors with aggressive adult T-cell leukemia/lymphoma. Leuk Res. 1993;17:157–66.
27. Kamihira S, Dateki N, Sugahara K, Hayashi T, Harasawa H, Minami S, et al. Significance of HTLV-1 proviral load quantification by real-time PCR as a surrogate marker for HTLV-1-infected cell count. Clin Lab Haematol. 2003;25:111–7.
28. Miyazato A, Kawakami K, Iwakura Y, Saito A. Chemokine synthesis and cellular inflammatory changes in lung of mice bearing p40tax of human T-lymphotropic virus type 1. Clin Exp Immunol. 2000;120:113–24.
29. Choi YL, Tsukasaki K, O'Neill MC, Yamada Y, Onimaru Y, Matsumoto K, et al. A genomic analysis of adult T-cell leukemia. Oncogene. 2007;26:1245–55.
30. Usui T, Yanagihara K, Tsukasaki K, Murata K, Hasegawa H, Yamada Y, et al. Characteristic expression of HTLV-1 basic zipper factor (HBZ) transcripts in HTLV-1 provirus-positive cells. Retrovirology. 2008;5:34–44.
31. Breems DA, Blokland EA, Neben S, Ploemacher RE. Frequency analysis of human primitive hematopoietic stem cell subsets using a cobblestone area forming cell assay. Leukemia. 1994;8:1095–104.
32. Satou Y, Yasunaga J, Yoshida M, Matsuoka M. HTLV-I basic leucine zipper factor gene mRNA supports proliferation of adult T cell leukemia cells. Proc Natl Acad Sci USA. 2006;103:720–5.
33. Mesnard JM, Barbeau B, Devaux C. HBZ, a new important player in the mystery of adult T-cell leukemia. Blood. 2006;108:3979–82.
34. Tomita K, van Bokhoven A, van Leenders GJ, Ruijter ET, Jansen CF, Bussemakers MJ, et al. Cadherin switching in human prostate cancer progression. Cancer Res. 2000;60:3650–4.
35. Alexander NR, Tran NL, Rekapally H, Summers CE, Glackin C, Heimark RL. *N-cadherin* Gene Expression in Prostate Carcinoma Is Modulated by Integrin-Dependent Nuclear Translocation of Twist1. Cancer Res. 2006;66:3365–9.
36. Williams TM, Lisanti MP. Caveolin-1 in oncogenic transformation, cancer, and metastasis. Am J Physiol Cell Physiol. 2005;288:494–506.
37. Paulsen MT, Starks AM, Derheimer FA, Hanasoge S, Li L, Dixon JE, et al. The p53-targeting human phosphatase hCdc14A interacts with the Cdk1/cyclin B complex and is differentially expressed in human cancers. Mol Cancer. 2006;5:25.
38. Mukhopadhyay D, Houchen CW, Kennedy S, Dieckgraefe BK, Anant S. Coupled mRNA Stabilization and Translational Silencing of Cyclooxygenase-2 by a Novel RNA Binding Protein, CUGBP2. Mol Cell. 2003;11:113–26.
39. Zhang X, Kim J, Ruthazer R, McDevitt MA, Wazer DE, Paulson KE, et al. The HBP1 transcriptional repressor participates in RAS-induced premature senescence. Mol Cellular Biol. 2006; 26:8252–66.

40. Rebollo A, Schmitt C. Ikaros, Aiolos and Helios: transcription regulators and lymphoid malignancies. Immunol Cell Biol. 2003;81:171–5.
41. Issaad C, Croisille L, Katz A, Vainchenker W, Coulombel M. A murine stromal cell line allows the proliferation of very primitive human CD34^{++}/CD38- progenitor cells in long-term cultures and semisolid assays. Blood. 1993;81:2916–24.
42. Bajénoff M, Egen JG, Koo LY, Laugier JP, Brau F, Glaichenhaus N, et al. Stromal cell networks regulate lymphocyte entry, migration, and territoriality in lymph nodes. Immunity. 2006; 25:989–1001.
43. Woolf E, Grigorova I, Sagiv A, Grabovsky V, Feigelson SW, Shulman Z, et al. Lymph node chemokines promote sustained T lymphocyte motility without triggering stable integrin adhesiveness in the absence of shear forces. Nat Immunol. 2007;8:1076–85.
44. Mitsiades CS, McMillin DW, Klippel S, Hideshima T, Chauhan D, Richardson PG, et al. The role of the bone marrow microenvironment in the pathophysiology of myeloma and its significance in the development of more effective therapies. Hematol Oncol Clin North Am. 2007;21:1007–34.
45. Lwin T, Hazlehurst LA, Dessureault S, Lai R, Bai W, Sotomayor E, et al. Cell adhesion induces p27Kip1-associated cell-cycle arrest through down-regulation of the SCFSkp2 ubiquitin ligase pathway in mantle-cell and other non-Hodgkin B-cell lymphomas. Blood. 2007;110:1631–8.
46. Tanaka Y, Kimata K, Wake A, Mine S, Morimoto I, Yamakawa N, et al. Heparan sulfate proteoglycan on leukemic cells is primarily involved in integrin triggering and its mediated adhesion to endothelial cells. J Exp Med. 1996;184:1987–97.
47. Imura A, Hori T, Imada K, Kawamata S, Tanaka Y, Imamura S, et al. OX40 expressed on fresh leukemic cells from adult T-cell leukemia patients mediates cell adhesion to vascular endothelial cells: implications for the possible involvement of OX40 in leukemic cell infiltration. Blood. 1997;89:2951–8.
48. Hiraiwa N, Hiraiwa M, Kannagi R. Human T-cell leukemia virus-1 encoded Tax protein transactivates alpha 1 → 3 fucosyltransferase Fuc-T VII, which synthesizes sialyl Lewis X, a selectin ligand expressed on adult T-cell leukemia cells. Biochem Biophys Res Commun. 1997;231:183–6.
49. Tanaka Y, Minami Y, Mine S, Hirano H, Hu CD, Fujimoto H, et al. H-Ras signals to cytoskeletal machinery in induction of integrin-mediated adhesion of T cells. J Immunol. 1999;163: 6209–16.
50. Sasaki H, Nishikata I, Shiraga T, Akamatsu E, Fukami T, Hidaka T, et al. Overexpression of a cell adhesion molecule, TSLC1, as a possible molecular marker for acute-type adult T-cell leukemia. Blood. 2005;105:1204–13.
51. Suzuki J, Fujita J, Taniguchi S, Sugimoto K, Mori KJ. Characterization of murine hematopoietic-supportive (MS-1 and MS-5) and non-supportive (MS-K) cell lines. Leukemia. 1992;6:452–8.
52. Tsuji T, Waga I, Tezuka K, Kamada M, Yatsunami K, Kodama H. Integrin beta2 (CD18)-mediated cell proliferation of HEL cells on a hematopoietic-supportive bone marrow stromal cell line, HESS-5 cells. Blood. 1998;91:1263–71.
53. Dewan MZ, Terashima K, Taruishi M, Hasegawa H, Ito M, Tanaka Y, et al. Rapid tumor formation of human T-cell leukemia virus type 1-infected cell lines in novel NOD-SCID/gammac(null) mice: suppression by an inhibitor against NF-kappaB. J Virol. 2003;77:5286–94.
54. Imada K, Takaori-Kondo A, Akagi T, Shimotohno K, Sugamura K, Hattori T, et al. Tumorigenicity of human T-cell leukemia virus type I-infected cell lines in severe combined immunodeficient mice and characterization of the cells proliferating in vivo. Blood. 1995;86:2350–7.
55. Hata T, Fujimoto T, Tsushima H, Murata K, Tsukasaki K, Atogami S, et al. Multi-clonal expansion of unique human T-lymphotropic virus type-1-infected T cells with high growth potential in response to interleukin-2 in prodromal phase of adult T cell leukemia. Leukemia. 1999;13:215–21.
56. Reya T, Morrison SJ, Clarke MF, Weissman IL. Stem cells, cancer, and cancer stem cells. Nature. 2001;414:105–11.
57. Bissell MJ, LaBarge MA. Context, tissue plasticity, and cancer: Are tumor stem cells also regulated by the microenvironment? Cancer Cell. 2005;7:17–23.
58. Gaudray G, Gachon F, Basbous J, Biard-Piechaczyk M, Devaux C, Mesnard JM. The complementary strand of the human T-cell leukemia virus type 1 RNA genome encodes a bZIP transcription factor that down-regulates viral transcription. J Virol. 2002; 76:12813–22.
59. Mori N, Fujii M, Ikeda S, Yamada Y, Tomonaga M, Ballard DW, et al. Constitutive activation of NF-kappaB in primary adult T-cell leukemia cells. Blood. 1999;93:2360–8.
60. Yamada Y, Nagata Y, Kamihira S, Tagawa M, Ichimaru M, Tomonaga M, et al. IL-2-dependent ATL cell lines with phenotypes differing from the original leukemia cells. Leukemia Res. 1991;15:619–25.

European Journal of Haematology ISSN 0902-4441

ORIGINAL ARTICLE

Foxp3 expression on normal and leukemic CD4$^+$CD25$^+$ T cells implicated in human T-cell leukemia virus type-1 is inconsistent with Treg cells

Masaki Abe[1,2], Kinya Uchihashi[2], Tsuruda Kazuto[1], Akemi Osaka[1], Katsunori Yanagihara[1], Kunihiro Tsukasaki[3], Hiroo Hasegawa[1], Yasuaki Yamada[1], Shimeru Kamihira[1]

[1]Department of Laboratory Medicine, Nagasaki University Graduate School of Biomedical Sciences, Nagasaki, Japan; [2]Sysmex Corporation, Wakinohama-Kaigandori, Chuo-ku, Kobe, Japan; [3]Department of Hematology, Nagasaki University Graduate School of Biomedical Sciences, Nagasaki, Japan

Abstract

Foxp3 is a master gene of Treg cells, a novel subset of CD4$^+$ T cells primarily expressing CD25. We describe here different features in Foxp3 expression profile between normal and leukemic CD4$^+$CD25$^+$ T cells, using peripheral blood samples from healthy controls (HCs), human T-cell leukemia virus type-1 (HTLV-1)-infected asymptomatic carriers (ACs), patients with adult T-cell leukemia (ATL), and various hematopoietic cell lines. The majority of CD4$^+$CD25$^+$ T cells in HCs were positive for Foxp3, but not all CD4$^+$CD25$^+$ T cells in ACs were positive, indicating that Foxp3 expression is not always linked to CD25 expression in normal T cells. Leukemic (ATL) T cells constitutively expressing CD25 were characteristic of heterogeneous Foxp3 expression, such as intra- and inter-case heterogeneity in intensity, inconsistency with CD25 expression, and a discrepancy in the mRNA and its protein expression. Surprisingly, a discernible amount of Foxp3 mRNA was detectable even in most cell lines without CD25 expression, a small fraction of which was positive for the Foxp3 proteins. The subcellular localization of Foxp3 in HTLV-1-infected cell lines was mainly cytoplasmic, different from that of primary ATL cells. These findings indicate that Foxp3 has two facets: essential Treg identity and molecular mimicry secondary to tumorigenesis. Conclusively, Foxp3 in normal T cells, but not mRNA, is basically potent at discriminating a subset of Treg cells from CD25$^+$ T-cell populations, whereas the modulation of Foxp3 expression in leukemic T cells could be implicated in oncogenesis and has a potentially useful clinical role.

Key words Foxp3; Treg; human T-cell leukemia virus type-1; adult T-cell leukemia; CD25

Correspondence S. Kamihira, PhD, MD, Department of Laboratory Medicine, Nagasaki University Graduate School of Biomedical Sciences, 1-7-1, Sakamoto, Nagasaki City, Japan 852-8501. Tel: +81 95 819 7407; Fax: +81 95 819 7422; e-mail: kamihira@nagasaki-u.ac.jp

Accepted for publication 22 May 2008

doi:10.1111/j.1600-0609.2008.01105.x

A forkhead box protein 3 (Foxp3) is noted as a novel T-cell marker identifying enigmatic Treg cells, and as a master gene regulating development and replication of the cells (1, 2). Recent studies of the scurfy mouse and the human immune dysregulation, polyendocrinopathy, enteropathy and X-linked syndrome (IPEX) models provide evidence that Foxp3 plays a major role in the differentiation of CD4$^+$CD25$^+$ Treg cells (3, 4). Foxp3 in mice has been shown to be exclusively expressed by only CD4$^+$CD25$^+$ Treg cells, designated as 'natural Treg cells' that are produced in the thymus through a homeostatic process. These findings from the mouse and human models indicate that Foxp3 is a master gene for development of Treg cells, representing a specific marker for identifying a cell lineage or a subset of Treg cells. In addition to natural Treg cells developing in the thymus, there is another type of Treg cells that acquire the Treg phenotype in mature cells because of antigen stimulation (5). Foxp3 gene transfection can also convert naïve CD4$^+$CD25$^-$ T cells into a regulatory phenotype expressing CD25 and

Foxp3, the so-called adaptive/inducible Treg cells (6, 7). Foxp3 expression is confirmed to be present in a minority of $CD4^+$ T-cell clones and $CD8^+$ T-cell clones, which are found exclusively in the activation populations (1). This suggests that Foxp3 expression is not always restricted to the natural Treg cell lineage and is inducible after T-cell activation.

Adult T-cell leukemia (ATL), which is a clonal lymphoproliferative neoplasm of post-thymic mature T cells, presents a $CD4^+CD25^+$ phenotype (8). ATL cells have the same markers as those of natural Treg cells, suggesting that ATL originates in natural Treg cells infected with human T-cell leukemia virus type 1 (HTLV-1). Recent studies (9, 10) have defined the presence of Foxp3 in ATL cells, but the oncological significance of Foxp3 in patients with ATL and asymptomatic HTLV-1 carriers (ACs) is controversial. Interestingly, HTLV-1, a causative retrovirus for ATL, has been reported to infect Treg cells and modulate the expression of Foxp3 (11–13). This suggests that Foxp3 is not only relevant as a surrogate molecule of Treg identity, but also likely involved in the oncogenesis of ATL. Accordingly, we investigated the expression profiles of both Foxp3 mRNA and proteins in normal and leukemic T cells expressing CD4 and CD25 in samples comprehensively collected from HTLV-1-seropositive people and ATL patients and various hematopoietic cell lines including HTLV-1-related lines. The clinical and oncological implications of alteration in Foxp3 expression are discussed.

Materials and methods

This study was performed under the approval of the Research Ethics Committee of our institute (no. 079260113). Peripheral blood mononuclear cells (PBMC) were obtained from blood samples of 24 patients with ATL (seven smoldering, five chronic, and 12 acute subtypes) and 48 normal control subjects by density gradient centrifugation using Lymphoprep (AXIS-SHIELD, Oslo, Norway). Normal controls were subdivided into healthy controls uninfected with HTLV-1, healthy controls (HCs), and asymptomatic HTLV-1 carriers (ACs). The subclassification of ATL was based on the criteria of Shimoyama *et al.* (14).

Cell lines

The cell lines used in this study included six interleukin (IL)-2-dependent ATL cell lines, ST1, KK1, KOB, SO4, LM-Y1 and OMT, two HTLV-1-infected T-cell lines, MT2 and HUT102, and 12 HTLV-1-negative T-cell lines, Jurkat, MOLT4, Raji, CA46, Ramos, U937, K562, THP1, SUDHL4, Cal-1, SKW6-4 and Daudi (15, 16). Cells were cultured in RPMI1640 medium with 10% fetal bovine serum (FBS). To culture IL-2-dependent cells, the medium was supplemented with 0.5 U/mL of IL-2 (kindly provided by Takeda Chemical Industries, Osaka, Japan).

Flow cytometric analysis of surface markers and intracellular Foxp3

Fluorescein isothiocyanate (FITC)-conjugated anti-CD25, and FITC- and phycoerythrin (PE)-conjugated mouse IgG1 as a negative control, and Periodimin–chlorophyll–protein complex (PerCP)-conjugated anti-CD4 monoclonal antibodies were purchased from BD Biosciences (San Diego, CA, USA). PE-conjugated anti-FOXP3 mAb (clone 236A/E7) was purchased from eBioscience (San Diego, CA, USA). PBMC and cell lines were first stained with anti-CD4 and anti-CD25 or FITC-conjugated mouse IgG1. Intracellular FOXP3 staining was achieved using a PE anti-human Foxp3 staining set (eBioScience) according to the manufacturer's instructions. Briefly, cells were fixed and permeabilized with fixation/permeabilization buffer including paraformaldehyde for 30 min at 4°C, and then stained with PE-conjugated anti-FOXP3 or PE-conjugated mouse IgG1 for 30 min at 4°C. Labeled cells were analyzed by flow cytometry with FACSCalibur (BD Bioscience).

PCR quantification for FOXP3

Total RNA was extracted using Isogen (NIPPONGENE, Toyama, Japan) according to the manufacturer's instructions. RNA was further purified by using MessageClean (GenHunter, Nashville, Germany). Total RNA (1 μg) was reverse transcribed using oligo(dT)18 primer and SuperScript III reverse transcriptase (Invitrogen, Carlsbad, CA, USA) and cDNA was synthesized. FOXP3 mRNA levels were quantified by real-time Polymerase chain reaction (PCR) using a commercially available primer set (Search-LC GmbH, Heidelberg, Germany), LightCycler-Primer Set Human Fox-P3 kit, and SYBR Green I Master kit (Roche, Mannheim, Germany) with the LightCycler 3.1 system (Roche). To ensure PCR quality, Porphobilinogen deaminase (PBGD) was measured in the same samples by a LightCycler-Primer Set Human PBGD. Cycling conditions were according to the manufacturer's instructions. As clinical samples consisted of a different mixture of Foxp3-positive and -negative cell populations, to compare the expression level of only $Foxp3^+$ cells, we adjusted by dividing the raw load by the percentage of $Foxp3^+$ cells, using the following formula: (Foxp3 copies)/(%$Foxp3^+$ cells) × 100.

To examine the full-length cDNA of Foxp3, conventional RT-PCR analysis was performed using the primer

set of 5′-GCTGATCCTTTTCTGTCAGTCC-3′ and 5′-GTGGAAACCTCACTTCTTGGTC-3′ for Foxp3. Amplification was established by Phusion™ Flash High-Fidelity DNA Polymerase (FINZYMES, Espoo, Finland). Cycling conditions were as follows: denaturation at 98°C for 30 s and at 98°C for 10 s, annealing and extension at 72°C for 45 s for 35 cycles, and extension at 72°C for 5 min for Foxp3. The PCR products were resolved on a 1.5% agarose gel, then visualized by ethidium bromide staining.

Western blot analysis and antibodies

Cells were harvested after treatment, washed, and homogenized at 4°C in a lysis buffer [0.1% sodium dodecyl sulfate (SDS), 1% Igepal CA-630, and 0.5% sodium deoxycholate] and a protease inhibitor cocktail (Sigma, St Louis, MO, USA). Cell lysates (30 μg) were resolved by electrophoresis on a 12.5% polyacrylamide gel and transferred to a polyvinylidine difluoride membrane. After blocking the membrane in 10% FBS and 0.1% Tween 20 in Tris-buffered saline for 1 h at room temperature, the blots were hybridized overnight at 4°C with primary antibodies. After hybridization with secondary antibodies conjugated with horseradish peroxidase, the immunocomplexes were visualized using an ECL Western blotting detection system (GE Healthcare, Chalfont St. Giles, UK). The analysis was performed using antibodies to an anti-FOXP3 monoclonal antibody (clone 236A/E7; eBioScience) and the monoclonal anti-β-actin antibody AC-15 (Sigma).

Immunocytochemistry for subcellular localization of Foxp3

Cells smeared on glass slides were fixed by 4% paraformaldehyde at 4°C for 15 min and then stained with PE-labeled anti-Foxp3 antibodies for 2 h at room temperature after permeabilization by the permeabilized commercial kit (BD Bioscience). The slides were counter-stained with Hoechst 33258 for staining of the nucleus and fluorescent conjugates of Lectin GS-II for selective staining of the Golgi apparatus (Molecular Probe Inc., Eugene, OR, USA). Signals were fluoroscopically observed using Leica DM400B Microsystems (Mannheim, Germany) and the fluorescence images were collected and analyzed with a Leica AF6000 Application Suite.

Statistical analysis

Using the STAT VIEW software, the Mann–Whitney *U*-test or Student's *t*-test was used to compare data between two groups, and Spearman's rank correlation was used to examine the two groups.

Results

Flow cytometric detection of Foxp3 proteins

Foxp3 expression was evaluated in normal and leukemic $CD4^+$ T cells by flow cytometric analysis. First, we examined the frequency of $CD25^+Foxp3^+$ cells in $CD4^+$ T cells from HCs, ACs, and patients with ATL and in various hematopoietic cell lines, as shown in Fig. 1. The mean percentage of $CD25^+Foxp3^+$ cells in $CD4^+$ T cells was not different between HCs and ACs (3.4 ± 1.7 vs. 3.1 ± 1.9), but the number of cells per milliliter in ACs was significantly lower ($1.5 \pm 0.4 \times 10^3$ vs. $1.1 \pm 0.3 \times 10^3$) than that in HCs ($P < 0.05$). There was no correlation between the percentage and aging. In patients with ATL, $CD25^+Foxp3^+$ cells were detectable at various frequencies from 1.5% to 84% in parallel to the presence of ATL cells defined by morphology, indicating that most ATL cells were positive for Foxp3. On the other hand, in contrast to Foxp3 expression on primary ATL cells, the expression of ATL-related cell lines was a weak fluorescent signal with a subtle shift to the right of relative fluorescence intensity (RFI). To confirm these flow cytometric findings of the Foxp3 stain, we studied fluoromicroscopically the subcellular localization profiles of Foxp3. As shown in Fig. 2, the Foxp3 red fluoro-spots were distributed diffusely in both the cytoplasm and the nucleus on primary ATL cells, and locally in the cytoplasm on ATL-related cell lines. To verify whether the localization of Foxp3 was associated with the Golgi apparatus in ATL-related cell lines, a co-localization experiment was performed using a lectin reactive for Golgi apparatus using the KOB cell line. As shown in Fig. 2 (KOB), the fluorescent red spots were

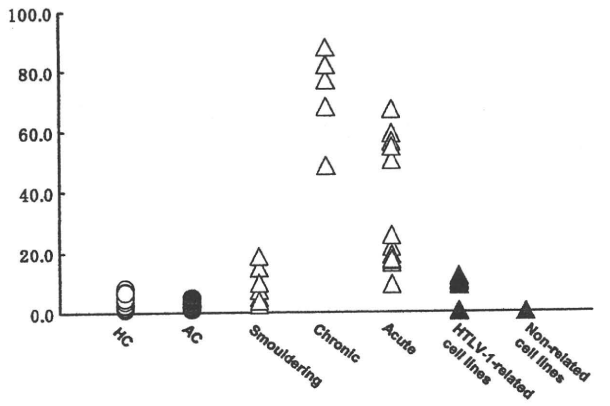

Figure 1 The frequency (%) of Foxp3-positive cells in $CD4^+$ T cells among healthy controls (HCs), human T-cell leukemia virus type-1 (HTLV-1)-infected asymptomatic carriers (ACs), patients with adult T-cell leukemia (ATL) and cell lines by flow cytometric analysis. The percentage in ATL cases was correlated with the number of leukemic ATL cells detected by morphological analysis.

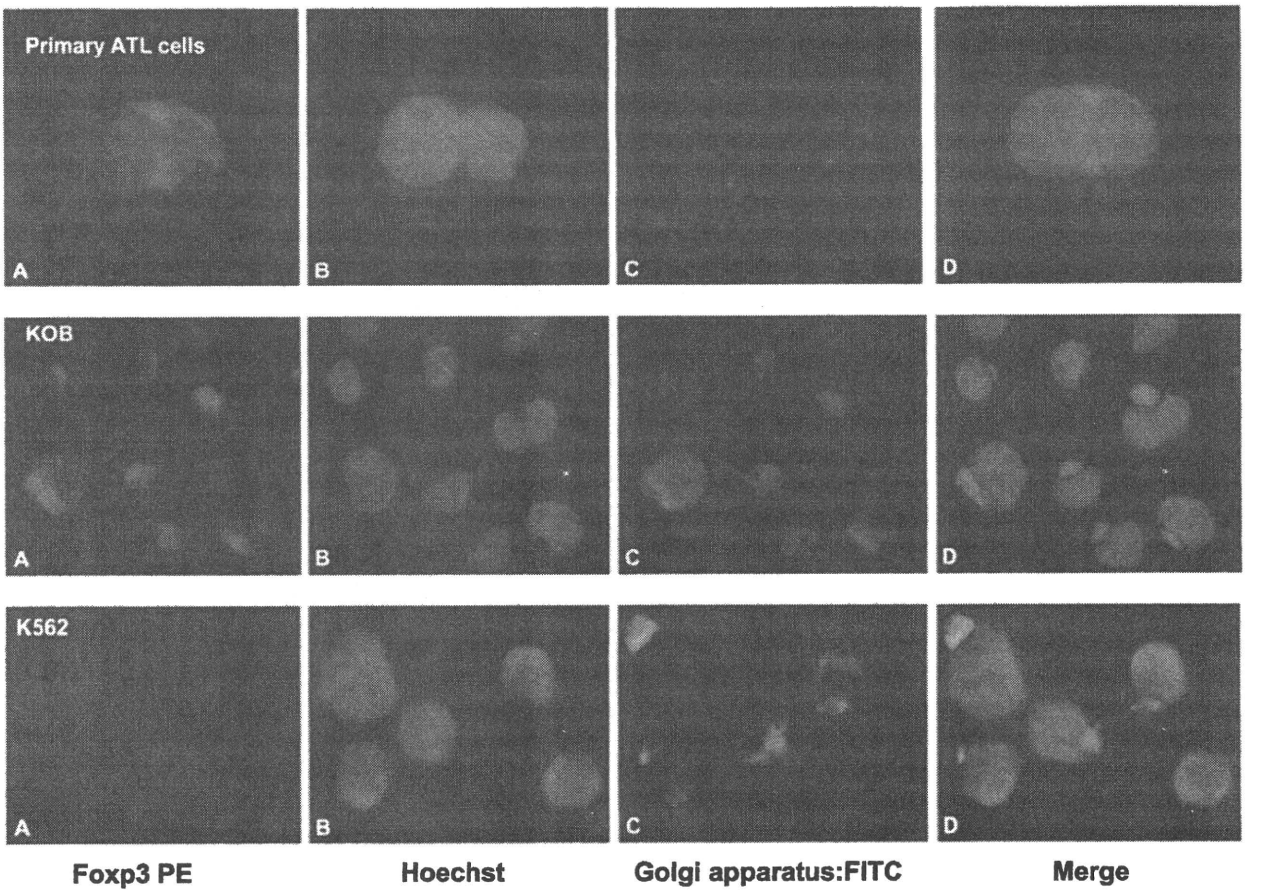

Figure 2 The subcellular localization of Foxp3 in primary ATL cells, KOB cells and K562 cells by immunocytochemistry. (A) Foxp3 staining (PE), (B) Hoechst stain, (C) lectin GS-II Golgi stain, (D) Merge. Although primary ATL cells and KOB cells shown here were positive for Foxp3 by flow-cytometric and Western blot analyses, immunocytochemistry revealed the different subcellular localizations, namely mainly nuclear in primary ATL cells and mostly cytoplasmic in KOB. K562 cells are negative control.

completely overlaid with the Golgi yellow spots, indicating that Foxp3 in KOB cells was colocalized within Golgi apparatus.

Then, according to the mutual expression profiles of CD25 and Foxp3 expression, $CD4^+$ cells were subdivided into four fractions: $CD25^+Foxp3^+$ (Treg-type), $CD25^+Foxp3^-$ (activated type), $CD25^-Foxp3^-$ (resting type), and $CD25^-Foxp3^+$ cells, as shown in Fig. 3. Most HCs showed the panel A pattern with a majority of $CD25^+$ cells co-expressing Foxp3, and most ACs showed the panel B pattern with a majority of $CD25^+$ cells not expressing Foxp3. On the other hand, the staining profile of primary ATL cells in ATL cases was variable, mainly a Treg-like pattern with weak CD25 and Foxp3 (panel C), and a mixed pattern of Treg-type cells and activated type $CD25^+$ cells (panel D and E). The intensity of CD25 in ATL cells was prone to decrease more than that of normal Treg cells. Then, to overview the relation of CD25 and Foxp3 expression in inter-cases, a twin plot graph was constructed as shown in Fig. 4, displaying the characteristic distribution in each group. Particularly, ATL cases (open triangles) were distributed in three main areas: cluster a, cases with $Foxp3^+$ cells = $CD25^+$ cells; b, cases with $Foxp3^+$ cells < $CD25^+$ cells; and c, cases with $Foxp3^+$ cell > $CD25^+$ cells.

Discrepant expression of Foxp3 in the mRNA and protein

Foxp3 mRNA was quantitatively detected in all 50 samples, regardless of the presence or absence of the proteins, and widely ranged from 700.0 to 1.0×10^5. These amplicons amplified by our system were confirmed to be concordant to that of nts 1190–1353 bp (NM014009) by sequencing analysis. The quantitative data in each sample (Fig. 5) show that there was no difference in the expression density among HCs, ACs, and patients with ATL, although patients with ATL tended to have a low mRNA dose. Notably, we were able to detect Foxp3 mRNA even in non-T cell lines, such as K562, Molt4,

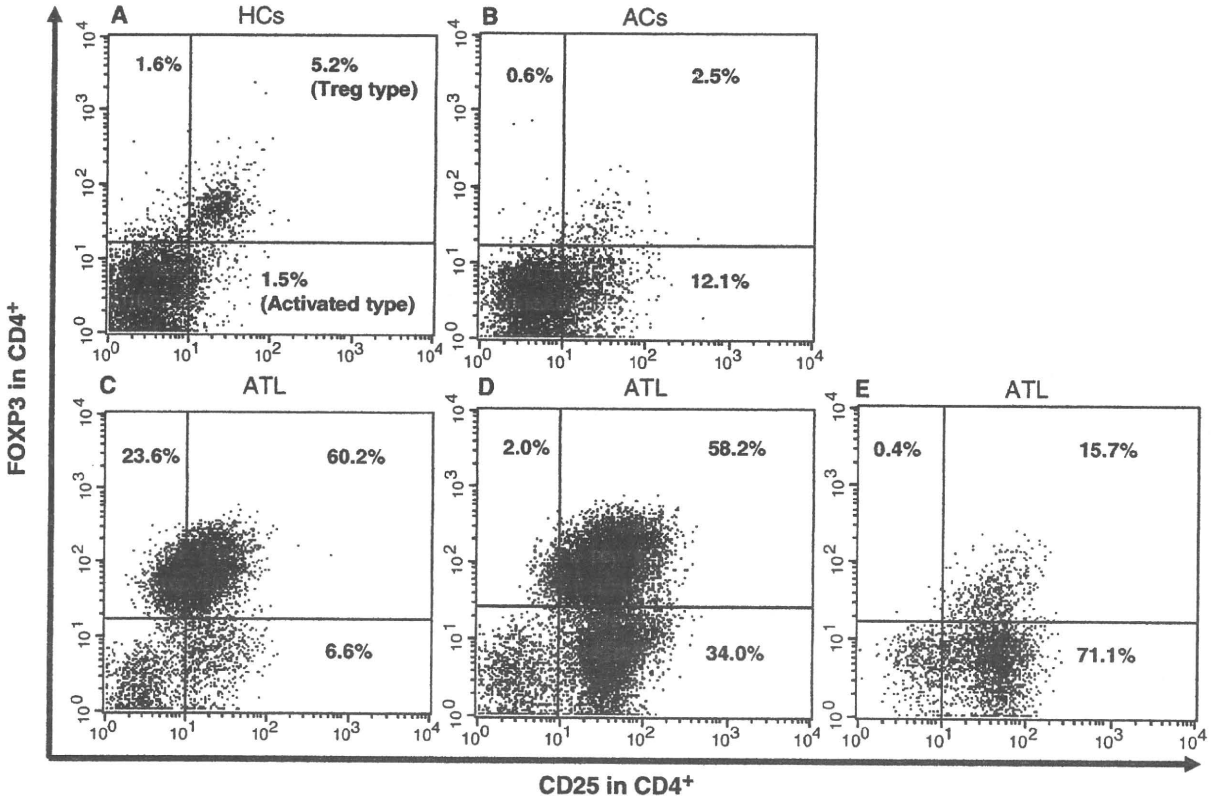

Figure 3 Representative triple staining patterns for CD4, CD25, and Foxp3 antigens. % – positive percentage for either Foxp3 or CD25 within $CD4^+$ T cells. (A) A representative case of HCs showing that most $CD25^+$ T cells co-expressed Foxp3 (Treg type). (B) A representative case of ACs showing that most $CD25^+$ T cells did not express Foxp3, i.e. they were activated $CD25^+$ cells. (C, D, and E) Variable ATL patterns showing heterogeneous Foxp3 expression inconsistent with CD25 expression in inter- and intra-case.

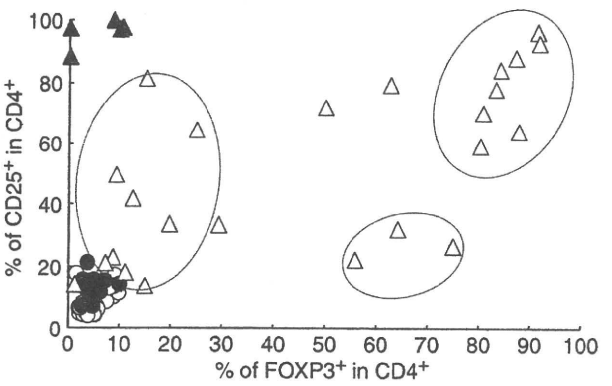

Figure 4 A twin dot-plot graph of $CD25^+$ cells (%) and $Foxp3^+$ cells (%) in each case. ATL (open triangle) is heterogeneously distributed with the main three clusters (broken line circles), while ATL-related cell lines (solid triangle) are concentrated in one area of $CD25^{high}$ and $Foxp3^{negative}$. HCs and ACs (open and solid circles) are localized at the same area, but ACs are prone to a shift toward the left side, indicating that the number of $CD25^+$cells is large compared with that of $Foxp3^+$cells.

Ramos, etc., despite no or subtle detection of Foxp3 proteins being demonstrable by flow cytometry. To confirm this discrepancy of the positive mRNA by PCR quantification and negative protein by flow cytometry, we reexamined by Western blot and RT-PCR analyses for full-length cDNA. As shown in Fig. 6, similar to that of the PCR quantification, equal amounts of two isoforms of Foxp3 [one corresponding to the full-length sequence and the other lacking exon 2 (17)] were detected in all samples, including non-T-cell lineage cell lines. On the other hand, Western blot analysis gave clear positive bands in KOB and LM-Y1 (lanes 5 and 6 in Fig. 6B) and a faint band in Ramos (lane 8). As described above, Foxp3 in KOB was demonstrated within the Golgi apparatus. These data on Foxp3 detection at the mRNA and protein levels by the different analyses in various cell lines are summarized in Table 1.

Discussion

First, our data showed that the majority of $CD4^+CD25^+$ T cells in HCs were positive for Foxp3,

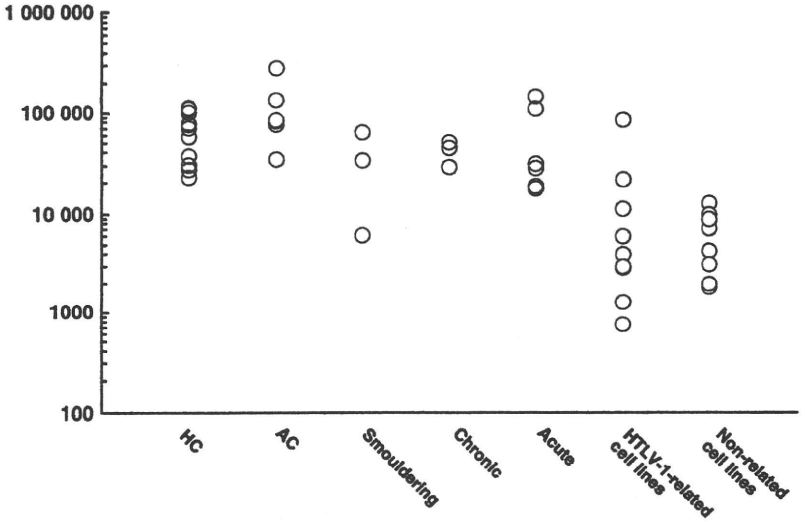

Figure 5 Comparison of the adjusted level of Foxp3 mRNA expression quantified by RT-PCR quantification among HCs, ACs, patients with ATL, HTLV-1-related T-cell lines, and HTLV-1-uninfected hematopoietic cell lines. No significant difference was observed among HCs, ACs and ATL patients, but the expression levels in the two groups of cell lines were significantly lower than those in the remaining three groups (the Mann–Whitney test).

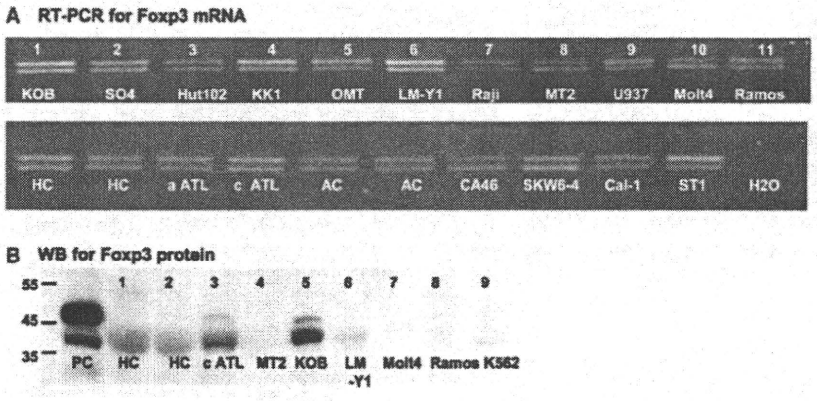

Figure 6 Conventional RT-PCR analysis for Foxp3 mRNA (A) and Western blot analysis (B). (A) The expected two bands (corresponding to full-length cDNA and splicing form) are observed in all samples tested. (B) Positive bands were observed in lanes 1, 2, 3, 5, and 6. PC, positive control derived from the manufacturer; HC, healthy control.

but not all $CD4^+CD25^+$ T cells in ACs were positive, indicating that Foxp3 expression is not always linked to CD25 expression in normal T cells. That is, $CD4^+CD25^+$ T cells in ACs were inconsistently composed of the two populations with or without Foxp3, suggesting that the former is Treg cells and the latter is either activated T cells or aberrant Treg cells downregulating Foxp3 expression. What does this imbalanced expression of CD25 and Foxp3 in ACs mean? Although we could not define whether the imbalance is a cause or an effect of HTLV-1 infections, Yamano *et al.* (18) reported the instructive finding that Foxp3 expression in $CD4^+CD25^+$ T cells from HAM patients was lower than those from HCs, and that Tax had a direct inhibitory effect on Foxp3 expression and function of $CD4^+CD25^+$ cells. This suggests that the imbalance of CD25 and Foxp3 expression in ACs is closely related to HTLV-1 infections. Moreover, this modulation of Foxp3 in the carrier stage may be causatively implicated in the frequent complications of autoimmune-like diseases, such as atopic dermatitis, myositis, Sjogren's syndrome and HTLV-1-associated uveitis (19). All of these clinical observations suggest that cell-mediated immunity is impaired in the HTLV-1 carriers. As for the underlying mechanism of impaired immunity, Yasunaga *et al.* reported that the unusual impaired cell-mediated immunity is likely explained by a decrease in naïve T cells and an increase in activated memory T cells (20). Although they did not examine Foxp3 expression at that time, the two points of our data and their data have something in common. That is, it is considered that the biological property of HTLV-1 through Tax misleads the immune reaction into immune disturbance with an imbalance in Treg and related cells. In the future, a study of both Foxp3 and HTLV-1 carriers could provide insights into the clinical role of Foxp3 as well as HTLV-1-associated immunopathology. Recently, Toulza *et al.* (21) reported the interesting findings that HTLV-1 infections are associated with abnormal expression of Foxp3 in circulating $CD4^+$cells and the efficacy of the immune control of HTLV-1 infection is mainly determined by the $CD4^+Foxp3^+Tax^-$ T-cell population.

Table 1 Summary of the Foxp3 and CD25 expression profile in various cell lines. Although Foxp3 mRNA was detected in all cell lines tested, Foxp3 protein was detected in only KOB and LM-Y1, all of which were established from adult T-cell leukemia cells

Cell lines	Lineage	Foxp3				CD25(%)	Tax
		FCM(%)	FCM(RFI)	WB	mRNA		
HTLV-1-related							
KOB	T	8.8	2.4	+	22 853	99.9	Moderate
LM-Y1	T	9.9	1.6	+	21 238	97.2	High
S04	T	1.7	1.2	−	1272	NT	Low
KK1	T	0.1	1.1	NT	83 801	88.5	Moderate
ST1	T	0.2	1.3	+/−	3879	97.4	Moderate
MT2	T	2.2	1.3	−	2970	98.9	High
OMT	T	10.6	1.9	+/−	734	97.7	High
HUT102	T	0.1	1.0	NT	5893	99.4	High
Non HTLV-1-related							
T1s	T	0.0	1.0	NT	10 958	0.0	
Jurkat	T	0.0	1.3	+/−	4182	0.0	
MOLT4	T	0.0	1.3	−	7144	0.1	
SKW6-4	T	NT	NT	NT	8763	0.0	
Raji	B	0.1	1.0	−	3102	0.0	
CA46	B	0.1	1.2	−	1948	0.0	
Ramos	B	NT	NT	+/−	9698	0.0	
Sudhl4	B	NT	NT	+/−	NT	0.0	
Daudi	B	0.0	1.2	NT	1350	0.0	
U937	Mono	0.1	1.2	−	12 408	0.0	
THP1	Mono	NT	NT	+/−	NT	0.0	
K562	M	0.0	1.0	+/−	1828	0.0	
Cal-1	DC	NT	NT	−	8430	0.0	
Samples							
HC		3.6	4.4	+	2489	9.2	
ACs		4.4	4.0	+	4827	13.4	
Primary ATL cells		87.0	4.3	+	24 927	96.5	

FCM (% and RFI), flow cytometric positive rate (%) and fluorescence intensity relative to the negative control (RFI).
WB: +, positive band; −, no band; +/−, faint band.
Tax: The expression level was subcategorized into the three groups, low, moderate and high, according to the PCR quantitative data.

As for leukemic $CD4^+CD25^+$ T cells, our data from ATL cells and ATL-related cell lines showed that Foxp3 expression is heterogeneous and aberrant, including intra- and inter-case heterogeneity in intensity, inconsistency with CD25 expression, and a discrepancy in the mRNA and its protein expression intensity. In particular, the difference in Foxp3 expression profiles between primary ATL cells and ATL-related cell lines is distinct and instructive. That is, the expression of CD25 and Foxp3 has an inverse relation; primary ATL cells are characteristic of weak CD25 and high Foxp3 intensity, while ATL-related cell lines have the distinct features of strong CD25 intensity and either negative or down-regulated Foxp3. The subcellular localization of Foxp3 is also different between them, mainly only cytoplasmic in the cell lines. This heterogeneous expression of Foxp3 in ATL attracts our attention to the origin of ATL cells and the implication of Foxp3 in ATL cell biology. With regard to the cell origin, although ATL originates from mature helper/inducer T cells, the recent focus has been directed at Treg cells because most ATL cells have the $CD25^+Foxp3^+$phenotype. Matsubara *et al.* (11) speculates on two possible mechanisms. One is a Treg cell origin, in which HTLV-1-infected Treg cells transform and modulate Foxp3 expression as a result of tumorigenesis, resulting in a Treg phenotype with heterogeneous Foxp3 expression. The other is an HTLV-1-infected $CD4^+CD25^-$ T cell origin, in which leukemic cells adaptively acquire the functional and phenotypical features similar to Treg, namely an inducible Treg-like feature. If an ATL cell is derived from primary Foxp3-expressing natural Treg cells, Foxp3 expression should be constitutive. However, our data that not all ATL cells are $Foxp3^+$cells and Foxp3 is ubiquitously detectable in various cell lines at least at the mRNA level appear to support the latter. Although the present study failed to identify that Tax is implicated in Foxp3 expression as an inducible factor, it is increasingly evident that Treg-like features are easily and frequently induced under pathological conditions in humans (22). However, at present decisive evidence is lacking. Accordingly, this does not rule out the other theory, and the two possibilities do

not seem to be mutually exclusive in the development of ATL.

Next, as for the oncological implication of Foxp3, our data showed that Foxp3 is not specific for ATL cells, because Foxp3, at least at the mRNA level, was detected in various cell lines derived from B cells, myeloid cells and dendritic cells. Indeed, some cases of T-chronic lymphocytic leukemia (12), cutaneous T-cell lymphoma and T-cell lymphoma carrying NPM-ALK (23) were reportedly positive for Foxp3. Furthermore, Foxp3 was reported to be positive even in solid tumors, such as pancreatic carcinomas (24). This ectopic expression beyond T-linearity suggests some implication of Foxp3 in tumorigenesis. From this point of view, a study by Hinz *et al.* (24) is interesting in that Foxp3 ectopically expressed in cancer cells plays a role of molecular mimicry as Treg function, representing a new mechanism of immune invasion in cancer. Similarly, our previous study showed that primary ATL cells expressing Foxp3 have the ability of anti-proliferative suppression for $CD4^+$ T cells in cell-to-cell contact manner (25). This Treg-like function in ATL cells appears to play a role in protecting them from immune attack and confers a survival advantage on ATL cells.

Conclusively, Foxp3 protein, but not mRNA, is basically potent at discriminating a subset of Treg cells from the population of normal $CD25^+$ T cells, whereas the modulation of Foxp3 in malignant cells is assuredly implicated in tumor pathology, indicating its potential as a new diagnostic and therapeutic molecule.

Acknowledgements

This study was supported financially by Japan Society for the Promotion of Science (no. 17390165 and no. 18659163).

References

1. Roncador G, Brown PJ, Maestre L, *et al.* Analysis of FOXP3 protein expression in human $CD4^+CD25^+$ regulatory T cells at the single-cell level. *Eur J Immunol* 2005;**35**:1681–91.
2. Read S, Powrie F. $CD4^+$ regulatory T cells. *Immunology* 2001;**13**:644–9.
3. Curiel T. Regulatory T-cell development: is Foxp3 the decider? *Nat Med* 2007;**13**:250–3.
4. Bennett CL, Christie J, Ramsdell F, Brunkow ME, Ferguson PJ, Whitesell L, Kelly TE, Saulsbury FT, Chance PF, Ochs HD. The immune dysregulation, polyendocrinopathy, enteropathy, X-linked syndrome (IPEX) is caused by mutations of FOXP3. *Nat Genet* 2001;**27**:20–1.
5. O'Garra A, Vieira P. Regulatory T cells and mechanisms of immune system control. *Nat Med* 2004;**10**:801–5.
6. Fontenot JD, Gavin MA, Rudensky AY. Foxp3 programs the development and function of $CD4^+CD25^+$ regulatory T cells. *Nat Immunol* 2003;**4**:330–6.
7. Hori S, Nomura T, Sakaguchi S. Control of regulatory T cell development by the transcription factor Foxp3. *Science* 2003;**299**:1057–61.
8. Matsuoka M. Human T-cell leukemia virus type I(HTLV-1) infection and the onset of adult T-cell leukemia(ATL). *Retrovirology* 2005;**2**:27 doi:10.1186/1742-4690-2-27.
9. Karube K, Ohshima K, Tsuchiya T, Yamaguchi T, Kawano R, Suzumiya J, Utsunomiya A, Harada M, Kikuchi M. Expression of FoxP3, a key molecule in CD4CD25 regulatory T cells, in adult T-cell leukaemia/lymphoma cells. *Br J Haematol* 2004;**126**:81–4.
10. Roncador G, Garcia JF, Garcia JF, Maestre L, Lucas E, Menarguez J, Ohshima K, Nakamura S, Banham AH, Piris MA. FOXP3, a selective marker for a subset of adult T-cell leukaemia/lymphoma. *Leukemia* 2005;**19**:2247–53.
11. Matsubara Y, Hori T, Morita R, Sakaguchi S, Uchiyama T. Phenotypic and functional relationship between adult T-cell leukemia cells and regulatory T cells. *Leukemia* 2005;**19**:482–3.
12. Matsubara Y, Hori T, Morita R, Sakaguchi S, Uchiyama T. Delineation of immunoregulatory properties of adult T-cell leukemia cells. *Int J Hematol* 2006;**84**:63–9.
13. Yamamoto M, Tsuji-Takayama K, Suzuki M, Harashima A, Sugimoto A, Motoda R, Yamasaki F, Nakamura S, Kibata M. Comprehensive analysis of FOXP3 mRNA expression in leukemia and transformed cell lines. *Leukemia Res* 2007;**32**:651–8.
14. Shimoyama M. Diagnostic criteria and classification of clinical subtypes of adult T-cell leukaemia-lymphoma. A report from the Lymphoma Study Group (1984-87). *Br J Haematol* 1991;**79**:428–37.
15. Yamada Y, Sugawara K, Hata T, *et al.* Interleukin-15 (IL-15) can replace the IL-2 signal in IL-2-dependent adult T-cell leukemia (ATL) cell lines: expression of IL-15 receptor alpha on ATL cells. *Blood* 1998;**91**:4265–72.
16. Hasegawa H, Yamada Y, Harasawa H, *et al.* Sensitivity of adult T-cell leukaemia lymphoma cells to tumor necrosis factor-related apoptosis-inducing ligand. *Br J Haematol* 2005;**128**:253–65.
17. Allan SE, Passerini L, Bacchetta R, Crellin N, Dai M, Orban PC, Ziegler SF, Roncarolo MG, Levings MK. The role of 2 FOXP3 isoforms in the generation of human $CD4^+$ Tregs. *J Clin Invest* 2005;**115**:3276–84.
18. Yamano Y, Takenouchi N, Li HC, Tomaru U, Yao K, Grant CW, Maric DA, Jacobson S. Virus-induced dysfunction of $CD4^+CD25^+$ T cells in patients with HTLV-I-associated neuroimmunological disease. *J Clin Invest* 2005;**115**:1144–6.
19. Matsuoka M. Human T-cell leukemia virus type I and adult T-cell leukemia. *Oncogene* 2003;**22**:5131–40.
20. Yasunaga JI, Sakai T, Nosaka K, Etoh Ki, Tamiya S, Koga S, Mita S, Uchino M, Mitsuya H, Matsuoka M.